PCCP

Accepted Manuscript

ROYAL SOCIETY OF CHEMISTRY

www.rsc.org/pccp

Deducing CO_2 Motion, Adsorption Locations and Binding Strengths in a Flexible Metal-Organic Framework without Open Metal Sites

Yue Zhang, Bryan E. G. Lucier, Yining Huang[a]

[a] *Department of Chemistry*

The University of Western Ontario

London, Ontario, Canada N6A 5B7

E-mail: yhuang@uwo.ca

Abstract

Microporous metal-organic frameworks (MOFs) have high surface areas and porosities, and are well-suited for CO_2 capture. MIL-53 features corner-sharing $MO_4(OH)_2$ (M = Al, Ga, Cr, etc.) octahedra interconnected by benzenedicarboxylate linkers that form one-dimensional rhombic tunnels, and exhibits an excellent adsorption ability for guest molecules such as CO_2. Studying the behavior of adsorbed CO_2 in MIL-53 via solid-state NMR (SSNMR) provides rich information on the dynamic motion of guest molecules as well as their binding strengths to the MOF host, and sheds light on the specific guest adsorption mechanisms. Variable-temperature ^{13}C SSNMR spectra of $^{13}CO_2$ adsorbed within various forms of MIL-53 are acquired and analyzed. CO_2 undergoes a combination of two motions within MIL-53; we report the type of motions present, their rates, and rotational angles. ^{1}H-^{13}C CP SSNMR experiments are used to examine the proximity of ^{1}H atoms in the MOF to ^{13}C atoms in CO_2 guests. By replacing ^{1}H for ^{2}H in MIL-53, the location of the CO_2 adsorption site in MIL-53 is experimentally confirmed by ^{1}H-^{13}C CP SSNMR. The binding strength of CO_2 within these MIL-53 MOFs follows the order MIL-53-NH_2 (Al) > MIL-53-NH_2 (Ga) > MIL-53 (Al) > MIL-53 (Ga).

Introduction

CO_2 emissions have increased dramatically in the past century due to the use of hydrocarbon fuels,[1] and accordingly, global warming has become a critical environmental issue. The development and use of specific materials for CO_2 capture and storage is a promising avenue for slowing or stopping global warming.[2, 3] Metal-organic frameworks (MOFs)[4-8] have great potential for CO_2 capture due to their high gas adsorption capacities and ability to selectively adsorb CO_2 from mixtures of different gases.[2, 9, 10] CO_2 capture in MOFs with coordinatively unsaturated open metal sites (*e.g.*, Mg-MOF-74/CPO-27-Mg) have been studied extensively using experimental[11-15] and computational[14-17] methods, however, MOFs without open metal sites have also demonstrated high CO_2 affinities when basic nitrogen-containing

organic groups (*e.g.* $-NH_2$)[18-22] or polarizing functional organic groups (*e.g.* –F, -Br, -Cl, -OH, -CN, $-NO_2$).[18, 21, 23-25] are incorporated into the linkers.

The MIL-53[26] (MIL= Materials of the Institute Lavoisier) series of MOFs has demonstrated the ability to adsorb CO_2 in significant quantities.[22, 27-30] The framework contains octahedral $MO_4(OH)_2$ (M= Al,[31] Cr,[26] Fe,[32] Ga,[33] In,[34] Sc[35]) secondary building units (SBUs) (Fig. 1(a)), which are composed of a metal center connected to four oxygen atoms from four different benzenedicarboxylate (BDC) ligands and two bridging hydroxyl oxygen atoms. These hydroxyl oxygen atoms link the SBUs *via* corner-sharing to form an infinite chain along the crystallographic *c*-axis (Fig 1(b)), and the chains are interconnected by BDC linkers to create one-dimensional rhombic channels (Fig 1(c)). It should be noted that the expensive nature of Ga, In and Sc metals render these variants of MIL-53 less practical alternatives in the context of using very large quantities of MOFs for CO_2 capture.

MIL-53 exhibits the ability to reversibly change phase and pore size in response to stimuli in a process known as the "breathing effect."[26] The magnitude of the breathing effect depends on the nature of metal center, functionalization of bridging ligands, external applied pressure, presence of guest molecules, and temperature.[36-39] Within as-made MIL-53 (MIL-53(*as*)), the rhombic pores measure 7.3 x 7.7 Å[31] and are occupied by excess BDC linkers from the MOF synthesis. At high temperature, the surplus BDC ligand is purged from the MOF channels to generate the high temperature phase MIL-53(*ht*), which has empty 8.5 x 8.5 Å pores.[31] MIL-53(*ht*) readily adsorbs water from air at room temperature to form the low temperature phase MIL-53(*lt*), which features narrow 2.6 x 13.6 Å pores.[31] The *lt-ht* phase transformation leads to an increase in unit cell volume of up to ca. 40%.[39]

MIL-53 exhibits an excellent affinity for CO_2. At 25 bar of pressure and a temperature of 304 K, MIL-53 (Al)(*ht*) can adsorb 30.6 wt% of CO_2, while at 1 bar and 298 K, MIL-53 (Al) can capture 10 wt% of CO_2.[30] Amino functionalized MIL-53 (NH_2-MIL-53(Al)) has also demonstrated significant CO_2 adsorption capacities. At 1 bar and 298 K, NH_2-MIL-53(Al) can capture 12 wt%

of CO_2,[29] while at 30 bar, it can adsorb 30 wt% of CO_2.[22] Prior computational studies have indicated the hydroxyl groups participating in the metal-oxygen-metal bond between SBUs are CO_2 adsorption sites in MIL-53.[28] With regards to the $–NH_2$ functional group, computational studies have indicated that there is no direct interaction of CO_2 and amine groups in NH_2-MIL-53,[27] however, the presence of amine groups on the framework linkers may influence the acidity of the bridging OH groups, and thus indirectly improve the adsorption ability.[27]

Solid-state NMR (SSNMR) provides detailed information on the short-range structural, magnetic, and electronic environment about a target nucleus. In the solid state, anisotropic (i.e., directionally-dependent) NMR interactions give rise to broad powder patterns of low signal-to-noise ratio (S/N), rather than the sharp resonances observed in solution NMR. These broad SSNMR spectra are often challenging to acquire, they contain rich information about the local environment and dynamics around the nucleus that may be unavailable from other characterization methods. SSNMR is often used in concert with complementary techniques such as powder X-ray diffraction (pXRD) to explore both the long- and short-range structure within a sample.[40, 41]

SSNMR has been employed for a multitude of purposes with respect to MOFs,[42-46] such as probing guest adsorption,[47-49] monitoring phase transformations,[50] determining the number and nature of non-equivalent atomic sites,[51] and examining the local environment of metal centers.[52, 53] CO_2 adsorbed in MOFs has recently been investigated via ^{13}C and ^{17}O SSNMR experiments,[45, 54-58] however, the dynamics of CO_2 within MOFs without open metal sites are not well-understood.[45, 58]

In this study, variable-temperature (VT) direct excitation ^{13}C and ^{1}H-^{13}C cross-polarization (CP) SSNMR experiments on $^{13}CO_2$-loaded MIL-53 (Al), MIL-53-NH_2 (Al), MIL-53 (Ga) and MIL-53-NH_2 (Ga) are used to investigate the dynamics of adsorbed CO_2 influenced by the metal center and functionalized amino groups. Static ^{13}C SSNMR spectra reveal that two distinct CO_2 motional modes are present within these MOFs. ^{1}H-^{13}C CP SSNMR experiments on deuterium

exchanged, $^{13}CO_2$-loaded MIL-53 samples are also employed to probe the specific location of CO_2 adsorption sites in this MOF. We now briefly explain our experimental approach and provide the fundamental basis as to why this approach provides unequivocal information about CO_2 dynamics and adsorption sites in MOFs.

The ^{13}C chemical shift is a local molecular property that is primarily dependent on the electron distribution in the CO_2 molecule, and can be modeled by a tensor with three perpendicular components (*vide infra*). The axial symmetry of the CO_2 molecule dictates that the one component of the CS tensor is directed along the O-C-O axis, while the other two components lie in the plane perpendicular to the O-C-O axis and pass through the ^{13}C nucleus. SSNMR experiments yield the magnitudes of each component of the chemical shift tensor and, by extension, richly illustrate the local environment about ^{13}C. In the context of CO_2 adsorption in MOFs, stationary CO_2 corresponds to a quantitatively predictable ^{13}C NMR lineshape with intensities in accordance with the distribution of CO_2 orientations in the polycrystalline sample. Any systematic, non-random dynamic motion of CO_2 about the molecular axis results in a quantitatively predictable averaging of the tensor components; even when two or more types of motions are simultaneously in play, the quantitative nature of the correspondence between the CO_2 motions and the resulting ^{13}C NMR lineshape is preserved.

Calculations to model the effect of dynamic motion on the NMR lineshape are well-known to the NMR community and conveniently performed using the EXPRESS software.[59] In this manner, determination of many specific details regarding the types and rates of CO_2 motion about the adsorption sites in MIL-53 is possible. We can also test the assumption that the CO_2 adsorption site in MIL-53 is specifically located at the bridging -OH group connecting the SBUs, by using a CP NMR experiment that relies on the proximity of ^1H nuclei in the framework and ^{13}C nuclei in adsorbed CO_2. This test involves replacing the ^1H nuclei of the bridging –OH groups with ^2H nuclei through deuterium exchange; the presence or lack of signal in ^1H-^{13}C CP NMR spectra will prove if the adsorption site for CO_2 is indeed close to the ^1H position on the bridging –OH groups.

Experimental Section

MOF synthesis. All chemicals were obtained from Sigma-Aldrich, and were used without further purification. MIL-53 (Al), NH_2-MIL-53 (Al), and MIL-53 (Ga) were synthesized using methods described in prior works (see ESI),[22, 31, 39] however, to the best of our knowledge, we are reporting the first hydrothermal synthesis of NH_2-MIL-53 (Ga).

NH_2-MIL-53 (Ga): $Ga(NO_3)_3 \cdot xH_2O$ (1.35 g, 5.30 mmol), 2-aminobenzene-1,4-dicarboxylic acid (1.50 g, 8.30 mmol) and 20 mL deionized H_2O were mixed into a 23 mL Teflon-lined stainless steel autoclave and heated at 150 ^oC for 3 days. The yellow powdered product was washed three times with deionized water and dried using vacuum filtration.

Sample activation. The activation process of MIL-53(*as*) consisted of first exchanging the trapped BDC organic linker with *N,N*-dimethylformamide (DMF) at high temperature in an autoclave overnight (*i.e.*, ≥ 12 h). For activation of MIL-53 (Al) and NH_2-MIL-53 (Al), 0.5 g of the as-made product and 10 mL of DMF were placed into a 23 mL Teflon-lined stainless steel autoclave and heated at 423 K. The DMF exchange of MIL-53 (Ga) and NH_2-MIL-53 (Ga) employed a heating temperature of 473 K. Following exchange of the BDC organic linker for DMF, all MOFs were heated at 473 K under dynamic vacuum (≤ 1 mbar) for 8 h to remove DMF molecules in the channels, yielding MIL-53(*ht*). In ambient conditions, MIL-53(*ht*) rapidly adsorbs water from the air to form MIL-53(*lt*).

Gas adsorption. A Schlenk line was used for gas adsorption experiments. The MIL-53(*lt*) sample was loaded into the bottom of a homemade 5 mm L-shaped glass tube. A thin layer of glass wool was used to secure the sample in place. The glass tube was attached to the Schlenk line and heated at 473 K for 8 h under dynamic vacuum to remove water from the MOF pores before gas loading. A known amount of pressurized $^{13}CO_2$ was then introduced to the vacuum line, and the CO_2 was allowed to occupy both the vacuum line and the glass tube containing the sample (82.7 cm^3). The bottom of the CO_2-filled glass tube was immersed in liquid nitrogen to freeze CO_2 within the sample, and the glass tube was then flame-sealed from the Schlenk line. The overall CO_2 loading amount is expressed by the molar ratio between CO_2 and the metal. In

this study, 0.2 CO_2/metal samples were prepared and characterized by SSNMR. Previous studies have shown that the maximum CO_2 loading amount in narrow-pore MIL-53 (Al) and NH_2-MIL-53 (Al, Ga) is ca. 0.5 CO_2/metal at 273 K,[30, 60] while our measured CO_2 adsorption isotherm (Supporting Information, Figure S7) indicates that the maximum amount of CO_2 that can be loaded in the narrow pore phase of MIL-53 (Ga) at 273 K is approximately 0.39 CO_2/metal. In that sense, this study employs a CO_2 loading level that is 40 % of the maximum loading possible in narrow-pore MIL-53(Al) and NH_2-MIL-53 (Al, Ga), and ca. 50 % of the maximum CO_2 capacity in narrow-pore MIL-53(Ga).

In the conditions employed in this study, all MIL-53 variants are expected to reside in the narrow-pore phase, as has been observed for both MIL-53-Al[30] and MIL-53-Sc[61] at the loading level of 0.2 CO_2/M. The study on MIL-53-Sc further explored changes in pore size associated with CO_2 loading, and found only a slight increase in pore size from 7.95 Å to 8.14 Å as the CO_2 loading level increased from 0.45 CO_2/M to 0.67 CO_2/M;[61] this ca. 2% difference in pore size with a ca. 50 % increase in CO_2 loading means that any pore distortions or expansion associated with our loading level of 0.20 CO_2/M are undoubtedly minor and should have a negligible effect on CO_2 dynamics in MIL-53 (Al, Ga). Our CO_2 adsorption isotherm of narrow-pore Ga-MIL-53 (Figure S7) also does not exhibit any evidence that a phase change from the narrow-pore phase or significant pore expansion has occurred when the pressure is lower than 1 bar.

Deuterium exchange in MIL-53. 0.1g MIL-53(*lt*) was immersed in 2 mL D_2O within a homemade 5 mm L-shaped glass tube for two days. During the exchange process, the glass tube was sealed with parafilm. The D_2O was extracted and replaced three times per day to ensure thorough deuteration of the sample. After D_2O exchange, the sample was activated and loaded with CO_2.

Powder X-ray diffraction. All pXRD patterns were acquired using an Inel CPS Powder Diffractometer operating with Cu Kα radiation. Reflections were collected at 2θ values between 5 and 120 degrees. All pXRD patterns are depicted in Fig. S1 of the ESI.

Solid-state NMR and the DEPTH-echo pulse sequence. SSNMR experiments were carried out on a Varian Infinity Plus spectrometer operating at a magnetic field of 9.4 T ($\nu_0(^{13}C)$ = 100.6 MHz) using a Varian/Chemagnetics 5 mm HX static probe. A Varian VT temperature control unit was used to adjust the temperature from 153 K to 393 K. Temperatures were measured to ± 2 K and calibrated using the ^{207}Pb chemical shift of $Pb(NO_3)_2$ (s) across the experimental temperature range.[62] All SSNMR spectra were acquired using the DEPTH-echo pulse sequence, which is the combination of both the DEPTH[63] and Hahn-echo pulse sequences. We have found that combining both the DEPTH and Hahn-echo features results in enhanced background signal suppression versus either individual pulse sequence in identical experimental times, especially when broad ^{13}C resonances are involved (Fig. S2 of the ESI).

A ^{13}C 90 ^{o} pulse length of 3.1 μs was employed for DEPTH-echo SSNMR experiments. The optimized ^{13}C pulse delays between scans were 7.5 s for MIL-53 (Al) and NH_2-MIL-53 (Al), and were 7 s for MIL-53 (Ga) and NH_2-MIL-53 (Ga). When the temperature was below 193 K, the optimized ^{13}C pulse delays of all sampless increased to 15 s. All spectra were acquired using a ^{1}H decoupling field of 81 kHz. For ^{1}H-^{13}C CP experiments, spectra with moderate (5 ms) and short (0.5 ms) contact times (CT) were acquired at temperatures of 173 K and 293 K. In the case of deuterium exchanged samples, only a CT of 5 ms was employed, since this allowed for observation of all resonances in ^{13}C powder patterns of all samples prior to deuterium exchange (*vide infra*, Results and Discussion). For deuterium exchanged MIL-53 (Al) and MIL-53 (Ga), the ^{1}H-^{13}C CP spectra were only collected at 173 K, because the ^{13}C SSNMR resonance corresponding to CO_2 component can only be observed at 173 K in the non-exchanged samples (*vide infra*), For deuterium exchanged NH_2-MIL-53 (Al) and NH_2-MIL-53 (Ga), the ^{1}H-^{13}C CP spectra were collected at both 173 K and 293 K, since the ^{13}C resonance corresponding to CO_2 can be observed at these two temperatures. ^{13}C SSNMR spectra were referenced to the resonance of methylene carbon in ethanol, which is located at ca. 58.05 ppm from TMS (tetramethylsilane).[64] The WSolids[65] computer software was used to obtain observed (i.e., apparent) NMR parameters, while the EXPRESS[59] software was used to simulate the

effects of CO_2 dynamics on ^{13}C SSNMR powder patterns and extract motional information.

The chemical shift (CS) interaction can be modeled by a tensor defined by three orthogonal components, δ_{11}, δ_{22}, and δ_{33}, which are ordered such that $\delta_{11} \geq \delta_{22} \geq \delta_{33}$. The isotropic chemical shift, δ_{iso}, is defined as $\delta_{iso} = (\delta_{11} + \delta_{22} + \delta_{33})/3$. The span of the CS tensor, Ω, describes the breadth of the powder pattern, and is the difference between the largest and smallest components of the CS tensor, $\Omega = \delta_{11} - \delta_{33}$. The skew of the CS tensor, κ, is defined as $\kappa = 3(\delta_{22} - \delta_{iso})/\Omega$. Values for κ range from −1 to +1, with either limit representing an axially symmetric CS tensor.

Results and Discussion

In this section, we present NMR results for CO_2 adsorbed in various MOFs, and analyze the ^{13}C SSNMR spectra in order to identify and understand the motional modes of CO_2. For readers who are not familiar with solid state NMR and uninterested in specific details, a brief summary of our findings in plain language is provided below.

Non-technical summary

The motion of CO_2 guests adsorbed within the MIL-53 (Al, Ga) and MIL-53-NH_2 (Al, Ga) series of MOFs has been investigated. In MIL-53, CO_2 simultaneously undergoes both a localized wobbling about the adsorption site, as well as a non-localized twofold hopping between the two equivalent adsorption sites. The wobbling and hopping motions occur through specific angles that depend on the metal center and functional groups incorporated in MIL-53. The wobbling and hopping angles in MIL-53-NH_2 are relatively small, indicating that –NH_2 functionalization of the linkers is associated with tighter, stronger binding of guest CO_2 molecules. The presence of Ga in MIL-53 is associated with larger CO_2 wobbling and hopping motional angles versus Al-based MIL-53, clearly demonstrating that the metal center has a strong influence on binding ability. The CO_2 binding strength in this series of MOFs is

summarized as follows: MIL-53-NH_2 (Al) > MIL-53-NH_2 (Ga) > MIL-53 (Al) > MIL-53 (Ga). The wobbling and hopping angles of CO_2 fall as temperature decreases. From the trend illustrated in Fig. 8, the wobbling and hopping angles will approach zero as the temperature drops to absolute zero (0 K). This is in good agreement with expectations from the crystal structure: when hopping is halted or frozen out, the occupancies of the two equivalent CO_2 adsorption sites would be 0.5. Our experiments unambiguously confirm that the CO_2 adsorption sites in MIL-53 are located on the bridging –OH groups linking MO_6 (M = Al, Ga) octahedra, in good agreement with predictions from previous computational studies.

Examining the dynamics of CO_2 within MIL-53 MOFs

The static ^{13}C SSNMR spectra of CO_2 adsorbed in MIL-53 (Al) at temperatures ranging from 153 K to 373 K (Fig. 2(a)) feature a broad powder pattern corresponding to adsorbed CO_2, which exhibits a temperature-dependent lineshape. The strong adsorption interaction between CO_2 and MIL-53 (Al) is reflected in the breadth of these chemical shift anisotropy (CSA) dominated powder patterns. Temperature-induced changes in the width and shape of the ^{13}C resonance are linked to the motion of adsorbed CO_2 within the MOF (*vide infra*).[55, 57] At high temperatures (*i.e.*, 313 to 353 K), a sharp resonance at ca. 125 ppm is also apparent; this signal is associated with unadsorbed CO_2, which has fast dynamics or has fast exchange with CO_2 inside the pore,[57] and is the only observed resonance at temperatures above 353 K.

The observed CS parameters of CO_2 in MIL-53 (Al) are summarized in Table 1. The apparent span (Ω) gradually decreases from 296(4) ppm to 223(1) ppm as the temperature increases from 153 K to 353 K. The observed skew (κ) also decreases from 0.99(1) to 0.60(1) as the temperature rises from 153 K to 353 K. With respect to the CS parameters of rigid CO_2 (Ω = 335 ppm, κ = 1),[66] the observation of smaller ^{13}C Ω values indicates that CO_2 within MIL-53 (Al) has increased motion at high temperatures, while the temperature-dependent κ values also confirm the presence of dynamic motion on the NMR timescale. Motionally-averaged NMR spectra may be simulated by the EXPRESS software,[59] which models the effect of dynamic

motion on NMR interactions and corresponding spectra. The EXPRESS-simulated ^{13}C SSNMR powder patterns of CO_2 within MIL-53 (Al) are shown in Fig. 2(b), and were obtained under the fast motion limit (*i.e.*, motional rates of $\geq 10^9$ Hz). The simulated powder patterns reveal that two types of dynamic CO_2 motions occur in this system: a six-fold (C_6) rotation and a two-fold (C_2) rotation. The C_6 rotation angle (α) varies from 12 ^{o} at 153 K to 21 ^{o} at 353 K, while the C_2 rotation angle (β) varies from 12 ^{o} to 24 ^{o} across the same temperature range. We propose that the C_6 rotation describes the localized wobbling of CO_2 molecules about the bridging hydroxyl group in MIL-53 (Fig. 3(a)), while the C_2 rotation describes the non-localized hopping of CO_2 between two separate bridging hydroxyl sites (Fig. 3(b) and 3(c)).

CO_2 wobbles through an angle α between the longitudinal axis of CO_2 and the wobbling axis (Fig. 3(a)). CO_2 hops along both the circumference of the channel in the *xy* plane (Fig. 3(c)) and along the length of the channel in the *z* direction. Previous computational studies have postulated that CO_2 molecules within MIL-53 and NH_2-MIL-53 interact with the bridging -OH groups of the SBUs at opposite sides of the channel.[27, 28] Our data experimentally confirms that CO_2 hops across the channel, alternating between two opposite CO_2 adsorption sites about an angle β between the longitudinal axis of CO_2 and the C_2 rotation axis (Fig. 3(b)). This type of hopping in the *xy* plane causes a reorientation of the ^{13}C CS tensor with respect to the molecule, influencing ^{13}C NMR powder patterns. In contrast, CO_2 hopping along the *z* direction is a translational motion that does not change the orientation of the ^{13}C CS tensors with respect to the molecule, therefore, CO_2 hops in the longitudinal direction (i.e., *z* direction) of the channel do not influence these ^{13}C SSNMR spectra. The combination of wobbling and hopping is shown in Fig. 3(d). Both the wobbling and hopping angles increase with temperature, indicating reduced CO_2 binding ability at high temperatures.

To explore the effect of a different metal center on CO_2 adsorption in MIL-53, the gallium analogue was investigated. The static ^{13}C SSNMR spectra of CO_2 adsorbed in MIL-53 (Ga) were acquired from 153 K to 393 K and are shown in Fig. 4(a). In this instance, a resonance

corresponding to unadsorbed mobile CO_2 was observed at temperatures above 313 K. Unlike MIL-53 (Al), the broad underlying ^{13}C powder pattern corresponding to adsorbed CO_2 in MIL-53 (Ga) is evident at temperatures above 353 K. These unique ^{13}C SSNMR observations arise because the magnitude of the breathing effect in MIL-53 depends on the metal center incorporated.[39] In MIL-53 (Al), the *lt* phase changes to the *ht* phase at 373 K, increasing the unit cell volume and pore size.[31] The larger pores and void space available in the *ht* phase discourages interactions between CO_2 and the adsorption site,[28] leading to the observation of unbound CO_2 in ^{13}C SSNMR experiments. In contrast, MIL-53 (Ga) only transitions to the *ht* phase when the temperature exceeds 493 K.[39] At 373 K and 393 K, narrow-pore MIL-53 (Ga) provides less mobility for CO_2, encouraging interaction with the adsorption sites within the MOF, and giving rise to a broad powder pattern.

The observed CS parameters of CO_2 within MIL-53 (Ga) exhibit a similar trend as CO_2 in MIL-53 (Al) (Table 1). As the temperature increases from 153 K to 393 K, Ω gradually decreases from 267(4) ppm to 191(1) ppm, and κ changes from 0.90(2) to 0.34(1). EXPRESS simulations of experimental ^{13}C powder patterns (Fig. 4(b)) reveal that CO_2 molecules are also dynamic in this system, undergoing localized wobbling and non-localized two-site hopping at a motional rate $\geq 10^9$ Hz in MIL-53 (Ga), which are strikingly similar to the CO_2 dynamics present in MIL-53 (Al) (Fig. 3(d)). The wobbling angle (α) increases from 18 ^{o} to 25 ^{o} and the hopping angle (β) climbs from 13 ^{o} to 28 ^{o} for CO_2 molecules in MIL-53 (Ga) as the temperature rises from 153 K to 393 K. At all temperatures, CO_2 adsorbed within MIL-53 (Ga) displays reduced apparent CS parameters and larger rotation angles versus CO_2 in MIL-53 (Al), indicating that CO_2 within MIL-53 (Ga) is more dynamic and is bound less tightly to the MOF. The difference in CO_2 binding ability between these two metal centers may be due to the different atomic radii. Larger atomic sizes can affect the metal-oxygen bond lengths and angles, which may influence the CO_2 binding strength associated with the bridging hydroxyl adsorption site.

Previous research has indicated that the presence of -NH_2 functional groups on the BDC

linkers within MIL-53 may enhance CO_2 capture ability.[22, 29] To study the effect of this amine functional group on CO_2 dynamics, static VT ^{13}C SSNMR spectra of CO_2 adsorbed within NH_2-MIL-53 (Al) were recorded at temperatures ranging from 153 K to 393 K (Fig. 5(a), Table 1). The broad CS powder patterns in the low temperature spectra of NH_2-MIL-53 (Al) are similar to those of MIL-53 (Al, Ga). A sharp resonance in the NH_2-MIL-53 (Al) spectrum corresponding to free CO_2 first emerges at 333 K, however, the intensity of this resonance at high temperatures is reduced compared to the resonance observed in MIL-53 (Al) and MIL-53 (Ga). The observed Ω values decrease from 309(4) ppm to 238(1) ppm as temperature increases from 153 K to 393 K. κ values also decrease as temperature increases, and κ is equal to 1 from 153 K to 193 K, corresponding to an axially symmetric CS tensor. In comparison with MIL-53 (Al), CO_2 adsorbed within NH_2-MIL-53 (Al) displays larger ^{13}C Ω and κ values, revealing that the presence of the $-NH_2$ functional group results in less dynamic CO_2 and stronger MOF-CO_2 binding.[27]

Simulations indicate that a C_6 wobbling and a C_2 hopping of CO_2 occur in NH_2-MIL-53 (Al) when the temperature is higher than 213 K (Fig. 5(b)). Since CO_2 is adsorbed at the same molecular sites in NH_2-MIL-53 (Al) and MIL-53 (Ga, Al),[27, 28] we propose that CO_2 within NH_2-MIL-53 (Al) undergoes the same type of motions: a localized wobbling on an individual adsorption site through a rotation angle of α, and a non-localized two-site (C_2) hopping through a rotation angle of β between adsorption sites (Fig. 3(d)). When the temperature is below 213 K, the C_2 hopping of CO_2 molecules is no longer apparent in ^{13}C SSNMR spectra of NH_2-MIL-53 (Al), leaving only the localized wobbling that is modeled by a C_6 rotation. The C_6 rotation angle (α), or wobbling angle, increases from 14 ^{o} to 20 ^{o} as the temperature rises from 153 K to 393 K, while the C_2 jumping angle (β) increases from 12 ^{o} to 20 ^{o} as the temperature increases from 213 K to 393 K. The presence of relatively small rotation angles across all temperatures, paired with the lack of C_2 hopping at low temperatures, reflect a much stronger CO_2 binding ability in NH_2-MIL-53 (Al) versus MIL-53 (Al, Ga).

In order to have a better understanding of the influence of metal center and functional group on gas adsorption, NH_2-MIL-53 (Ga) was also studied. Static ^{13}C SSNMR spectra of adsorbed CO_2 within NH_2-MIL-53 (Ga) were acquired in the temperature range from 153 K to 393 K (Fig. 6(a)). A narrow central ^{13}C resonance corresponding to free CO_2 is apparent at room temperature and dominates the spectrum at high temperatures, indicating that the MOF has a relatively low CO_2 adsorption capacity and binding strength in the context of this study. This decreased CO_2 adsorption capacity may be due to the reduction of available surface area: the BET surface area of NH_2-MIL-53 (Ga) is only 210 m^2/g,[67] which is far below the BET surface area of MIL-53 (Ga) (1230 m^2/g).[67] The decreased binding strength associated with CO_2 adsorption may be due to the Ga metal center used in this variant of NH_2-MIL-53: a larger atomic size can also affect the metal-oxygen bond lengths and angles, which may influence the CO_2 binding strength associated with the bridging hydroxyl adsorption site in NH_2-MIL-53.

The observed ^{13}C CS parameters of adsorbed CO_2 in NH_2-MIL-53 (Ga) decrease as temperature increases (Table 1). Ω values decrease from 289(3) to 230(1) ppm as the temperature rises from 153 K to 393 K, while κ diminishes from 0.97(2) at 153 K to 0.70(1) at 393 K. The observed Ω and κ values in NH_2-MIL-53 (Ga) are larger than those in MIL-53 (Ga), but smaller than those in NH_2-MIL-53 (Al), indicating that CO_2 dynamics and MOF-CO_2 binding strength in NH_2-MIL-53 (Ga) lie between those observed in MIL-53 (Ga) and NH_2-MIL-53 (Al).

EXPRESS simulations (Fig. 6(b)) again show that two type of CO_2 motions (Fig. 3(d)) are present: a localized C_6 wobbling and a non-localized C_2 jumping. The C_6 wobbling angle, α, varies from 16 ^{o} at 153 K to 22 ^{o} at 393 K, while the C_2 hopping angle β increases from 10 ^{o} at 153 K to 21 ^{o} at 393 K. CO_2 adsorbed within NH_2-MIL-53 (Ga) exhibits both wobbling and hopping even at low temperatures. The increased dynamics of CO_2 versus within NH_2-MIL-53 (Al) indicates that the nature of the metal center plays a role in guest adsorption, likely due to the influence of the specific metal center on the binding ability of the bridging OH groups between SBUs.

The graphs in Fig. 7 and Fig. 8 provide a comparison of ^{13}C CS parameters and rotation angles within all four MIL-53 variants. The ^{13}C CS parameters are related to the motion of CO_2 within MOFs; CO_2 molecules moving through larger wobbling angles are generally linked to reduced Ω values,[57] and in this case, the κ value is intimately related to the hopping angle. In the MIL-53 and NH_2-MIL-53 MOFs, larger CO_2 hopping angles correspond to smaller κ values. CO_2 adsorbed within NH_2-MIL-53 (Al) exhibits the largest Ω and κ values observed under any acquired temperature, while CO_2 in MIL-53 (Ga) is linked to the smallest Ω and κ values (Fig. 7). The interpretation of these findings is that CO_2 within MIL-53-NH_2 (Al) is bound tightest and undergoes a relatively small amount of dynamic motion, while CO_2 within MIL-53 (Ga) is bound weakest and undergoes increased dynamics. Amine functionalization of the linkers in MIL-53 (Al, Ga) leads to the observation of smaller CO_2 motional angles (α and β) in comparison to ordinary MIL-53 (Fig. 8), indicating that CO_2 is adsorbed more strongly and exhibits reduced dynamics when the MIL-53 linker is functionalized with the NH_2 group. It is important to again note that the metal center has a clear influence on CO_2 binding ability in all variations of MIL-53. CO_2 adsorbed in MIL-53 (Ga) is more dynamic than CO_2 adsorbed in MIL-53 (Al), and CO_2 adsorbed in NH_2-MIL-53 (Ga) exhibits enhanced dynamics versus CO_2 adsorbed in NH_2-MIL-53 (Al).

The results in Fig. 8 display a trend that agrees well with rational expectations. The compromise between increasing kinetic energy at higher temperatures versus the net attractive adsorption energy results in an increasing C_6 rotation angle with temperature. Although the NMR parameters were acquired across a 250 °C range, the trend is to approach ca. 0 degrees in both hopping and wobbling angles at absolute zero, as it should. There are two symmetrically equivalent adsorption sites within one MIL-53 cavity; at the limit of 0 K, Fig. 8 suggests the hopping motion would be frozen out and the occupancies of the two equivalent sites would be 0.5.

Studying the interaction of CO_2 with adsorption sites

SSNMR experiments employing cross polarization (CP) from ^{1}H to ^{13}C were employed to study the adsorption strength between CO_2 guests and the MIL-53 host. CP experiments are mediated by dipolar coupling and, by extension, internuclear distance;[68] this dependence can be exploited to obtain detailed information on the spatial proximity between nuclei. The contact time (CT) in CP experiments describes the period of time that CP is allowed to occur. With longer CTs, polarization across longer internuclear distances can typically be transferred, and when shorter CTs are employed, only ^{13}C nuclei that are relatively proximate to ^{1}H will be detected. In this instance, ^{1}H-^{13}C CP experiments have been employed to explore the location of the CO_2 adsorption sites in MIL-53, which have been postulated to be proximate to the hydroxyl group joining SBUs.[27, 28]

In MIL-53 (Al), ^{1}H-^{13}C CP SSNMR experiments were employed on both the empty framework and CO_2-loaded samples (Fig. 9(a)). The ^{13}C resonances observed in the empty framework arise from carbon atoms in the BDC linkers. Hydrogen is directly bound to carbon in BDC, therefore, ^{1}H polarization is efficiently transferred to ^{13}C, resulting in a very strong resonance. The use of long and short CTs in ^{1}H-^{13}C CP SSNMR experiments on the CO_2-loaded sample at room temperature results in similar spectra, which both resemble those of the empty framework. The absence of a ^{13}C resonance corresponding to adsorbed CO_2 at 293 K in ^{1}H-^{13}C CP SSNMR spectra of MIL-53 (Al) is due to the long hydroxyl ^{1}H-$^{13}CO_2$ distance and the highly dynamic motion of CO_2 molecules, which rapidly modulate and dephase the weak dipolar couplings. At 173 K, the intensity of the highest frequency peak in CP spectra (denoted * in Fig. 9(a)) is enhanced versus room temperature spectra when both long and short CTs are employed. This high frequency resonance is located approximate to the δ_{11} component of the ^{13}C CS tensor from adsorbed CO_2 detected *via* ^{13}C DEPTH-echo SSNMR spectra at the same temperature (Fig. 2), and indeed represents adsorbed CO_2. At low temperatures, the CO_2 molecule is less dynamic, preserving the dipolar coupling between the adsorption site and CO_2, and permitting the detection of adsorbed CO_2 by ^{1}H-^{13}C CP experiments.

^{1}H-^{13}C CP SSNMR experiments were also performed on empty MIL-53 (Ga) and CO_2-loaded MIL-53 (Ga) samples (Fig. 9(b)). The room temperature ^{1}H-^{13}C CP SSNMR spectra of CO_2-loaded MIL-53 (Ga) resemble the CP spectra of the empty framework when both long and short CTs are used, indicating that the CO_2 molecule undergoes very fast dynamic motion, and that there may be a relatively long ^{1}H-$^{13}CO_2$ distance at this temperature. The CO_2 resonance is only apparent at 173 K when a long CT is employed, indicating a weaker ^{1}H-^{13}C dipolar interaction between CO_2 molecule and the adsorption site in MIL-53 (Ga) compared with MIL-53 (Al) at this temperature, this data supports the interpretation that CO_2 is bound weaker in MIL-53 (Ga) than in MIL-53 (Al).

The ^{1}H-^{13}C CP SSNMR spectra of NH_2-MIL-53 (Al, Ga) feature ^{13}C resonances corresponding to both the framework and adsorbed CO_2 at room temperature, even when short CTs are employed (Fig. 10). These findings confirm that a strong dipolar interaction exists between CO_2 guests and the adsorption site within the amine-functionalized versions of MIL-53. CO_2 molecules are bound more strongly and exhibit reduced dynamics versus non-functionalized MIL-53 (Al, Ga). At low temperatures, the intensity of the resonance corresponding to adsorbed CO_2 is enhanced, in agreement with the stronger binding strength indicated by low temperature ^{13}C DEPTH-echo SSNMR experiments. Previous research has shown that there is no direct interaction of CO_2 and the amine functional groups in these systems,[27] therefore, the enhancement of the resonance linked to adsorbed CO_2 must be due to an increase in the dipolar coupling strength between hydrogen atoms from the adsorption site and carbon from adsorbed CO_2. These ^{1}H-^{13}C CP SSNMR experimental results clearly show that the presence of an amino group enhances the binding strength between CO_2 guests and the MIL-53 host.

To probe the specific location of CO_2 adsorption sites within MIL-53, ^{1}H-^{13}C SSNMR CP experiments were performed on deuterium-exchanged MIL-53 samples. Since ^{2}H cannot participate in ^{1}H-^{13}C CP experiments, ^{13}C nuclei proximate to ^{2}H are not detected. It has been

observed that the H atom in –OH groups can be easily exchanged by ^{2}H in $^{2}H_2O$.[69, 70] Previous studies have indicated that the bridging –OH group which connects SBUs in MIL-53 is the CO_2 adsorption site.[27, 28] In a deuterium exchanged MIL-53 sample, only the ^{1}H atoms on the bridging –OH group are replaced by ^{2}H, forming a $–O^{2}H$ hydroxyl group. In this manner, the CO_2 adsorption site may be inferred from the success or failure of ^{1}H-^{13}C CP experiments on deuterium-exchanged MIL-53.

Since the ^{13}C powder pattern corresponding to adsorbed CO_2 within MIL-53 (Al) and MIL-53 (Ga) could only be detected in ^{1}H-^{13}C CP SSNMR spectra at 173 K in non-deuterated samples, ^{1}H-^{13}C SSNMR CP experiments on deuterium exchanged MIL-53 (Al, Ga) were only performed at 173 K (Fig. 11). The only ^{13}C resonances present in the ^{1}H-^{13}C CP SSNMR spectra of the deuterium exchanged MIL-53 samples correspond to the BDC linker of the MOF; the resonance corresponding to adsorbed CO_2 is not present. The ^{1}H-^{13}C dipolar interaction between the framework adsorption sites and adsorbed CO_2 in deuterium exchanged MIL-53 samples is absent due to the deuteration of the –OH group connecting the SBUs. These ^{1}H-^{13}C CP SSNMR spectra provide strong proof that the bridging –OH group between SBUs is the CO_2 adsorption site within MIL-53.

The ^{1}H-^{13}C CP SSNMR spectra of deuterium exchanged NH_2-MIL-53 (Al, Ga) samples at 293 K (Fig. 11) are very similar to those of the empty frameworks, suggesting that ^{1}H-^{13}C dipolar coupling between CO_2 and the adsorption site within the MOF is absent. Interestingly, at 173 K, ^{1}H-^{13}C CP SSNMR spectra of deuterated NH_2-MIL-53 (Al, Ga) feature a resonance corresponding to adsorbed CO_2 (denoted * in Fig. 12), however, the intensity of this CO_2-linked resonance is low, while the intensity of framework ^{13}C resonances is relatively high. These spectra indicate that weak ^{1}H-^{13}C dipolar couplings between CO_2 carbon atoms and hydrogen are present at low temperature in deuterium exchanged NH_2-MIL-53 (Al) and NH_2-MIL-53 (Ga). Unfortunately, in MIL-53-NH_2, the hydrogen atoms associated with the $–NH_2$ amino group may also participate in fast deuterium exchange,[71, 72] hence, ^{1}H-^{13}C CP SSNMR experiments alone

cannot distinguish whether the CO_2 adsorption site in deuterated NH_2-MIL-53 lies on the linker amino group or the SBU –OH moiety.[27] The weak ^1H-^{13}C dipolar interactions at this temperature could also involve the carbon atom of CO_2 molecule and ^1H atoms located on the BDC linker. Since the NH_2-MIL-53 is associated with a narrower pore size than MIL-53,[27, 73] short distances between CO_2 and the benzene ring of the BDC linker may be possible, permitting a weak ^1H-^{13}C dipolar interaction.

Conclusions

^{13}C SSNMR experiments have been used to probe the CO_2 dynamics and binding strength within a MOF without open metal sites. CO_2 guests in MIL-53 (Al, Ga) and NH_2-MIL-53 (Al, Ga) undergo both a localized wobbling and a non-localized hopping between two separate adsorption sites. Simulations of experimental SSNMR data provide the rates and angles associated with each type of motion. All of the motional angles increase with temperature from 153 K to 393 K. These ^{13}C SSNMR spectra reveal that differences in CO_2 binding strength among the various MIL-53 MOFs are linked to (i) the nature of the metal center and (ii) the presence of functional groups on the BDC linkers. The relatively weaker CO_2 binding interaction in non-functionalized MIL-53 results in increased CO_2 mobility. ^1H-^{13}C CP SSNMR experiments indicate that CO_2 binding strength in MIL-53 is influenced by the nature of the metal center and the presence of functional groups. ^1H-^{13}C CP SSNMR spectra of deuterated MIL-53 suggests that the bridging hydroxyl groups between metal centers serve as the CO_2 adsorption sites within MOFs.

Our work provides a clear picture of CO_2 dynamics in MIL-53, and advances the understanding of gas adsorption in MOFs without open metal sites. Detailed knowledge and understanding of the dynamics in this series of MOFs should unlock avenues for modifications to existing and future MOFs in order to improve the CO_2 wt % uptake at a given temperature,

working towards the goal of long-term CO_2 capture and sequestration in MOFs. More detailed SSNMR studies are currently being performed to probe the fine details underpinning CO_2 adsorption within the MIL-53 series of MOFs. *Ab initio* calculations are another complementary avenue that can accurately predict NMR parameters associated with gases adsorbed in MOFs;[74] this route should allow detailed analysis of individual contributions to NMR parameters and assist in fully characterizing CO_2 adsorption and dynamics in the MIL-53 system.

Acknowledgments

Y.H. thanks The Natural Sciences and Engineering Research Council of Canada (NSERC) for a Discovery Grant and a Discovery Accelerator Supplements Award.

References

1. R. Quadrelli and S. Peterson, *Energy Policy*, 2007, **35**, 5938-5952.
2. K. Sumida, D. L. Rogow, J. A. Mason, T. M. McDonald, E. D. Bloch, Z. R. Herm, T. H. Bae and J. R. Long, *Chem. Rev.*, 2012, **112**, 724-781.
3. D. M. D'Alessandro, B. Smit and J. R. Long, *Angew. Chem.-Int. Edit.*, 2010, **49**, 6058-6082.
4. H. Zhou and S. Kitagawa, *Chem. Soc. Rev.*, 2014, **43**, 5415-5418.
5. H. Furukawa, K. E. Cordova, M. O'Keeffe and O. M. Yaghi, *Science*, 2013, **341**, 974.
6. H. Zhou, J. R. Long and O. M. Yaghi, *Chem. Rev.*, 2012, **112**, 673-674.
7. J. L. C. Rowsell and O. M. Yaghi, *Micropor. Mesopor. Mat.*, 2004, **73**, 3-14.
8. S. L. James, *Chem. Soc. Rev.*, 2003, **32**, 276-288.
9. Z. Zhang, Y. Zhao, Q. Gong, Z. Li and J. Li, *Chem. Commun.*, 2013, **49**, 653-661.
10. J. Li, Y. Ma, M. C. McCarthy, J. Sculley, J. Yu, H.-K. Jeong, P. B. Balbuena and H. Zhou, *Coord. Chem. Rev.*, 2011, **255**, 1791-1823.
11. C. Montoro, E. Garcia, S. Calero, M. A. Perez-Fernandez, A. L. Lopez, E. Barea and J. A. R. Navarro, *J. Mater. Chem.*, 2012, **22**, 10155-10158.

12. J. A. Mason, K. Sumida, Z. R. Herm, R. Krishna and J. R. Long, *Energy Environ. Sci.*, 2011, **4**, 3030-3040.

13. Y. G. Lee, H. R. Moon, Y. E. Cheon and M. P. Suh, *Angew. Chem.-Int. Edit.*, 2008, **47**, 7741-7745.

14. P. Canepa, N. Nijem, Y. J. Chabal and T. Thonhauser, *Phys. Rev. Lett.*, 2013, **110**.

15. L. Valenzano, B. Civalleri, S. Chavan, G. T. Palomino, C. O. Areán and S. Bordiga, *J. Phys. Chem. C*, 2010, **114**, 11185-11191.

16. P. Canepa, C. A. Arter, E. M. Conwill, D. H. Johnson, B. A. Shoemaker, K. Z. Soliman and T. Thonhauser, *J. Mater. Chem. A*, 2013, **1**, 13597-13604.

17. L. Valenzano, B. Civalleri, K. Sillar and J. Sauer, *J. Phys. Chem. C*, 2011, **115**, 21777-21784.

18. G. E. Cmarik, M. Kim, S. M. Cohen and K. S. Walton, *Langmuir*, 2012, **28**, 15606-15613.

19. S. Choi, T. Watanabe, T. H. Bae, D. S. Sholl and C. W. Jones, *J. Phys. Chem. Lett.*, 2012, **3**, 1136-1141.

20. R. Vaidhyanathan, S. S. Iremonger, G. K. H. Shimizu, P. G. Boyd, S. Alavi and T. K. Woo, *Science*, 2010, **330**, 650-653.

21. A. Torrisi, R. G. Bell and C. Mellot-Draznieks, *Cryst. Growth Des.*, 2010, **10**, 2839-2841.

22. S. Couck, J. F. M. Denayer, G. V. Baron, T. Remy, J. Gascon and F. Kapteijn, *J. Am. Chem. Soc.*, 2009, **131**, 6326-6327.

23. Y. Huang, W. Qin, Z. Li and Y. Li, *Dalton Trans.*, 2012, **41**, 9283-9285.

24. T. Devic, F. Salles, S. Bourrelly, B. Moulin, G. Maurin, P. Horcajada, C. Serre, A. Vimont, J. C. Lavalley, H. Leclerc, G. Clet, M. Daturi, P. L. Llewellyn, Y. Filinchuk and G. Ferey, *J. Mater. Chem.*, 2012, **22**, 10266-10273.

25. Q. Yang, A. D. Wiersum, P. L. Llewellyn, V. Guillerm, C. Serred and G. Maurin, *Chem. Commun.*, 2011, **47**, 9603-9605.

26. C. Serre, F. Millange, C. Thouvenot, M. Nogues, G. Marsolier, D. Louer and G. Ferey, *J. Am. Chem. Soc.*, 2002, **124**, 13519-13526.

27. E. Stavitski, E. A. Pidko, S. Couck, T. Remy, E. J. M. Hensen, B. M. Weckhuysen, J. Denayer, J. Gascon and F. Kapteijn, *Langmuir*, 2011, **27**, 3970-3976.

28. N. A. Ramsahye, G. Maurin, S. Bourrelly, P. L. Llewellyn, C. Serre, T. Loiseau, T. Devic and G. Ferey, *J. Phys. Chem. C*, 2008, **112**, 514-520.

29. B. Arstad, H. Fjellvag, K. O. Kongshaug, O. Swang and R. Blom, *Adsorpt.-J. Int. Adsorpt. Soc.*, 2008, **14**, 755-762.

30. S. Bourrelly, P. L. Llewellyn, C. Serre, F. Millange, T. Loiseau and G. Ferey, *J. Am. Chem. Soc.*, 2005, **127**, 13519-13521.

31. T. Loiseau, C. Serre, C. Huguenard, G. Fink, F. Taulelle, M. Henry, T. Bataille and G. Ferey, *Chem.-Eur. J.*, 2004, **10**, 1373-1382.

32. T. R. Whitfield, X. Q. Wang, L. M. Liu and A. J. Jacobson, *Solid State Sci.*, 2005, **7**, 1096-1103.

33. M. Vougo-Zanda, J. Huang, E. Anokhina, X. Q. Wang and A. J. Jacobson, *Inorg. Chem.*, 2008, **47**, 11535-11542.

34. E. V. Anokhina, M. Vougo-Zanda, X. Q. Wang and A. J. Jacobson, *J. Am. Chem. Soc.*, 2005, **127**, 15000-15001.

35. J. P. S. Mowat, V. R. Seymour, J. M. Griffin, S. P. Thompson, A. M. Z. Slawin, D. Fairen-Jimenez, T. Duren, S. E. Ashbrook and P. A. Wright, *Dalton Trans.*, 2012, **41**, 3937-3941.

36. P. Serra-Crespo, A. Dikhtiarenko, E. Stavitski, J. Juan-Alcaniz, F. Kapteijn, F. X. Coudert and J. Gascon, *Crystengcomm*, 2015, **17**, 276-280.

37. S. Biswas, T. Ahnfeldt and N. Stock, *Inorg. Chem.*, 2011, **50**, 9518-9526.

38. T. Devic, P. Horcajada, C. Serre, F. Salles, G. Maurin, B. Moulin, D. Heurtaux, G. Clet, A. Vimont, J. M. Greneche, B. Le Ouay, F. Moreau, E. Magnier, Y. Filinchuk, J. Marrot, J. C. Lavalley, M. Daturi and G. Ferey, *J. Am. Chem. Soc.*, 2010, **132**, 1127-1136.

39. C. Volkringer, T. Loiseau, N. Guillou, G. Ferey, E. Elkaim and A. Vimont, *Dalton Trans.*, 2009, 2241-2249.

40. C. Martineau, *Solid State Nucl. Magn. Reson.*, 2014, **63-64**, 1-12.

41. W. R. E. Harris R. K., Duer M. J., *NMR Crystallography*, John Wiley & Sons Ltd., U.K., 2009.

42. Y. Huang, Xu, J., Gul-E-Noor, F., He, P., *Encyclopedia of Inorganic and Bioinorganic Chemistry, Vol. 1*, John Wiley & Sons, Ltd., Chichester, UK 2014.

43. S. E. Ashbrook, D. M. Dawson and V. R. Seymour, *Phys. Chem. Chem. Phys.*, 2014, **16**, 8223-8242.

44. A. Sutrisno and Y. Huang, *Solid State Nucl. Magn. Reson.*, 2013, **49-50**, 1-11.

45. H. C. Hoffmann, M. Debowski, P. Muller, S. Paasch, I. Senkovska, S. Kaskel and E. Brunner, *Materials*, 2012, **5**, 2537-2572.

46. J. Xu , B. E. G. Lucier , R. Sinelnikov, V. V. Terskikh, V. N. Staroverov and Y. Huang, *Chem. Eur. J.*, 2015, DOI: 10.1002/chem.201501954.

47. D. I. Kolokolov, H. Jobic, S. Rives, P. G. Yot, J. Ollivier, P. Trens, A. G. Stepanov and G. Maurin, *J. Phys. Chem. C*, 2015, **119**, 8217-8225.

48. C. Lieder, S. Opelt, M. Dyballa, H. Henning, E. Klemm and M. Hunger, *J. Phys. Chem. C*, 2010, **114**, 16596-16602.

49. B. Ibrahim, B. E. G. Lucier, J. Xu, P. He and Y. Huang, *Can. J. Chem.* 2015, **93**, 960-969.

50. M.-A. Springuel-Huet, A. Nossov, Z. Adem, F. Guenneau, C. Volkringer, T. Loiseau, G. Férey and A. Gédéon, *J. Am. Chem. Soc.*, 2010, **132**, 11599-11607.

51. J. Xu, V. V. Terskikh and Y. Huang, *Chem.-Eur. J.*, 2013, **19**, 4432-4436.

52. P. He, J. Xu, V. V. Terskikh, A. Sutrisno, H. Y. Nie and Y. Huang, *J. Phys. Chem. C*, 2013, **117**, 16953-16960.

53. A. Sutrisno, V. V. Terskikh, Q. Shi, Z. Song, J. Dong, S. Ding, W. Wang, B. R. Provost, T. D. Daff, T. K. Woo and Y. Huang, *Chem.-Eur. J.*, 2012, **18**, 12251-12259.

54. W. D. Wang, B. E. G. Lucier, V. V. Terskikh, W. Wang and Y. Huang, *J. Phys. Chem. Lett.*, 2014, **5**, 3360-3365.

55. L. Lin, J. Kim, X. Kong, E. Scott, T. M. McDonald, J. R. Long, J. A. Reimer and B. Smit, *Angew. Chem.-Int. Edit.*, 2013, **52**, 4410-4413.

56. F. Gul-E-Noor, M. Mendt, D. Michel, A. Poppl, H. Krautscheid, J. Haase and M. Bertmer, *J. Phys. Chem. C*, 2013, **117**, 7703-7712.

57. X. Kong, E. Scott, W. Ding, J. A. Mason, J. R. Long and J. A. Reimer, *J. Am. Chem. Soc.*, 2012, **134**, 14341-14344.

58. M. Peksa, S. Burrekaew, R. Schmid, J. Lang and F. Stallmach, *Micropor. Mesopor. Mat.*, 2015, **216**, 75-81.

59. R. L. Vold and G. L. Hoatson, *J. Magn. Reson*, 2009, **198**, 57-72.

60. P. Serra-Crespo, E. Gobechiya, E. V. Ramos-Fernandez, J. Juan-Alcañiz, A. Martinez-Joaristi, E. Stavitski, C. E. A. Kirschhock, J. A. Martens, F. Kapteijn and J. Gascon, *Langmuir*, 2012, **28**, 12916-12922.

61. L. Chen, J. P. S. Mowat, D. Fairen-Jimenez, C. A. Morrison, S. P. Thompson, P. A. Wright and T. Düren, *J. Am. Chem. Soc.*, 2013, **135**, 15763-15773.

62. C. Dybowski and G. Neue, *Prog. Nucl. Mag. Res. Sp.*, 2002, **41**, 153-170.

63. D. G. Cory and W. M. Ritchey, *J. Magn. Reson*, 1988, **80**, 128-132.

64. H. E. Gottlieb, V. Kotlyar and A. Nudelman, *J. Org. Chem.*, 1997, **62**, 7512-7515.

65. R. E. W. K. Eichele, *WSolids1*, University of Tübingen, Tübingen, Germany, 2001.

66. A. J. Beeler, A. M. Orendt, D. M. Grant, P. W. Cutts, J. Michl, K. W. Zilm, J. W. Downing, J. C. Facelli, M. S. Schindler and W. Kutzelnigg, *J. Am. Chem. Soc.*, 1984, **106**, 7672-7676.

67. J. Canivet, J. Bonnefoy, C. Daniel, A. Legrand, B. Coasne and D. Farrusseng, *New J. Chem.*, 2014, **38**, 3102-3111.

68. M. J. Duer, *Solid-State NMR Spectroscopy Principles and Applications*, Blackwell Science, Oxford, 2002.

69. J. H. Stewart, R. H. Shapiro, C. H. Depuy and V. M. Bierbaum, *J. Am. Chem. Soc.*, 1977, **99**, 7650-7653.

70. L. M. Jackman and S. Sternhell, *Applications of Nuclear Magnetic Resonance Spectroscopy in Organic Chemistry (Second Edition)*, Pergamon Press Ltd., Oxford U. K., 1969.

71. J. R. Hanson, *The Organic Chemistry of Isotopic Labelling*, Royal Society of Chemistry, Cambridge, UK, 2011.

72. D. L. Pavia, G. M. Lampman, G. S. Kriz and J. A. Vyvyan, *Introduction to Spectroscopy, Fourth Edition*, Brooks Cole, Belmont, USA, 2008.

73. P. Serra-Crespo, M. A. van der Veen, E. Gobechiya, K. Houthoofd, Y. Filinchuk, C. E. A. Kirschhock, J. A. Martens, B. F. Sels, D. E. De Vos, F. Kapteijn and J. Gascon, *J. Am. Chem. Soc.*, 2012, **134**, 8314-8317.

74. M. G. Lopez, P. Canepa and T. Thonhauser, *J. Chem. Phys.*, 2013, **138**, 154704.

Table 1. The observed, or apparent, ^{13}C CS parameters of CO_2 adsorbed within MIL-53, as obtained from analytical simulations of static ^{13}C DEPTH-echo variable temperature SSNMR spectra.[a]

T	MIL-53 (Al)			MIL-53 (Ga)			NH_2-MIL-53 (Al)			NH_2-MIL-53 (Ga)		
	δ_{iso} (ppm)[b]	Ω (ppm)[c]	κ[d]	δ_{iso} (ppm)	Ω (ppm)	κ	δ_{iso} (ppm)	Ω (ppm)	κ	δ_{iso} (ppm)	Ω (ppm)	κ
393 K				124(1)	191(1)	0.34(1)	124(1)	238(1)	0.76(1)	122(1)	230(1)	0.70(1)
373 K				125(1)	191(1)	0.35(1)	125(1)	251(1)	0.79(1)	123(1)	230(1)	0.72(1)
353 K	125(1)	223(1)	0.60(1)	125(1)	194(1)	0.39(1)	125(1)	250(1)	0.80(1)	127(1)	236(1)	0.74(1)
333 K	125(1)	234(2)	0.70(1)	124(1)	198(2)	0.41(1)	124(1)	257(2)	0.84(1)	126(1)	239(1)	0.75(1)
313 K	125(1)	243(2)	0.76(1)	124(1)	201(2)	0.46(1)	124(2)	259(2)	0.87(1)	125(1)	239(2)	0.77(1)
293 K	126(1)	246(2)	0.78(1)	123(1)	204(2)	0.51(1)	123(2)	266(2)	0.90(1)	123(1)	247(2)	0.80(1)
273 K	126(1)	250(2)	0.83(1)	124(2)	208(2)	0.57(1)	123(2)	268(3)	0.92(1)	127(1)	248(2)	0.82(1)
253 K	126(1)	258(2)	0.86(1)	125(2)	218(2)	0.61(1)	122(2)	275(3)	0.94(1)	126(1)	254(2)	0.84(1)
233 K	126(1)	263(3)	0.90(1)	125(2)	228(3)	0.66(1)	122(2)	277(3)	0.97(1)	126(2)	261(2)	0.87(1)
213 K	126(2)	266(3)	0.94(1)	125(2)	236(3)	0.73(1)	123(3)	277(3)	0.99(1)	127(1)	264(3)	0.90(1)
193 K	126(2)	278(3)	0.96(1)	125(2)	247(3)	0.79(1)	120(3)	297(4)	1.00(1)	124(2)	274(3)	0.92(2)
173 K	126(2)	287(4)	0.98(1)	125(2)	256(3)	0.86(2)	122(3)	299(4)	1.00(1)	125(2)	282(3)	0.94(2)
153 K	125(2)	296(4)	0.99(1)	125(2)	267(4)	0.90(2)	124(3)	309(4)	1.00(1)	125(2)	289(3)	0.97(2)

[a]The uncertainties in δ_{iso}, Ω, and κ were measured from experimental spectra and corresponding simulations. [b]Isotropic chemical shift: $\delta_{iso} = (\delta_{11} + \delta_{22} + \delta_{33})/3$. [c]Span: $\Omega = \delta_{11} - \delta_{33}$. [d]Skew: $\kappa = 3(\delta_{22} - \delta_{iso})/\Omega$

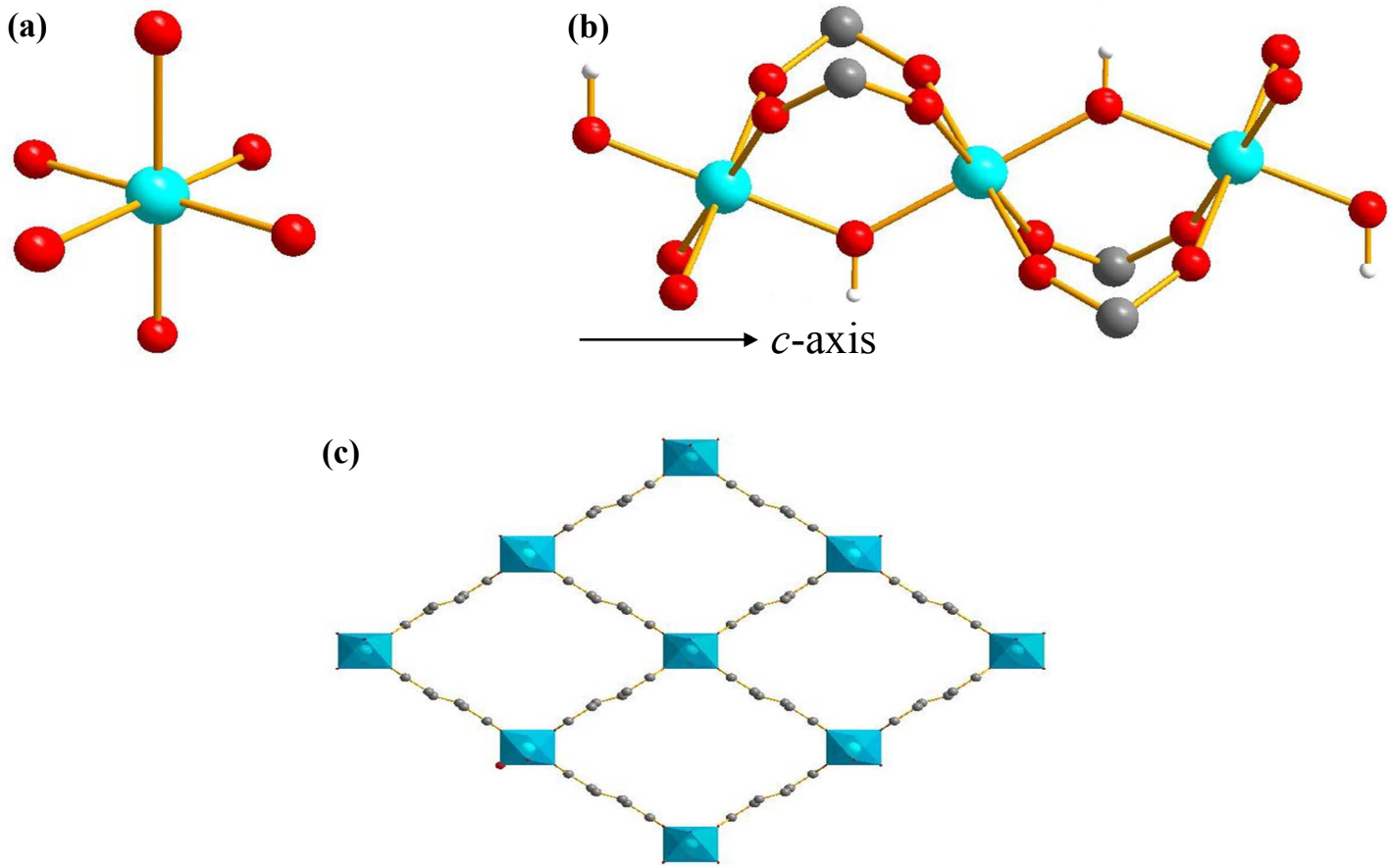

Fig. 1 The octahedral $MO_4(OH)_2$ secondary building unit (SBU) of the MIL-53 MOF is shown in (a). The chain formed by the SBUs along the crystallographic *c* axis is shown in (b); these chains are interconnected by benzenedicarboxylate (BDC) linkers to create the one-dimensional rhombic channels, as shown in (c). The colors red, grey, white and blue correspond to oxygen, carbon, hydrogen and the metal center, respectively.

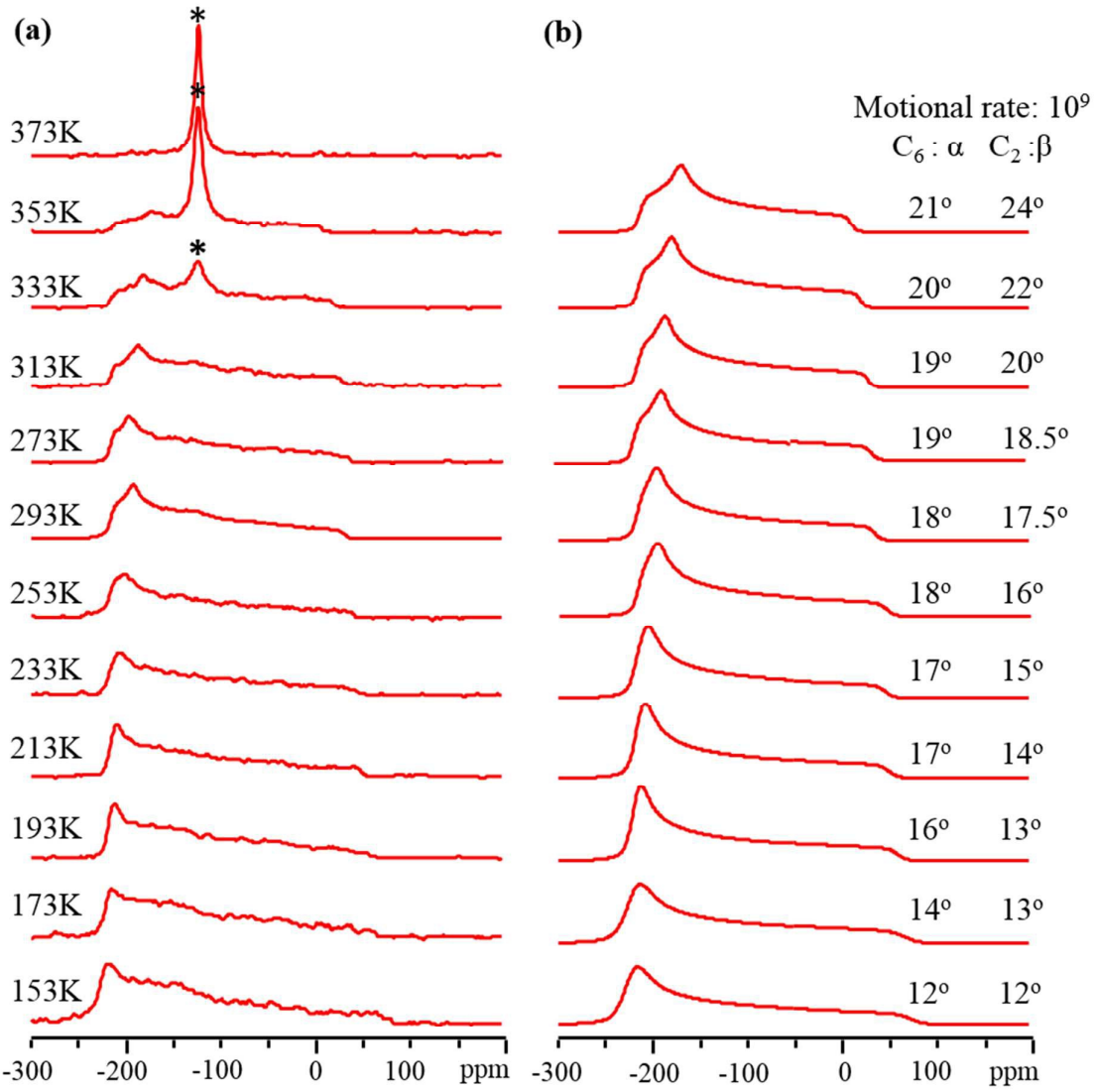

Fig. 2 The experimental and simulated static ^{13}C SSNMR spectra of adsorbed CO_2 within MIL-53 (Al) are shown in (a) and (b) respectively. The simulated powder patterns were generated using the EXPRESS software and a fast rate of motion (10^9 Hz) for both dynamic modes. The C_6 motion (six-fold rotation) and accompanying angle α describe the localized wobbling of CO_2 about the adsorption site (see Fig. 3a), while the C_2 motion and β refer to a non-localized two-fold hopping between two adsorption sites (see Fig. 3b and 3c). The asterisk (*) denotes a sharp resonance at high temperature that corresponds to gaseous, unbound CO_2. See Figure S3 (ESI) for uncropped spectra that clearly show the edges of each powder pattern. The uncertainty in α and β is estimated to be ± 0.5 °.

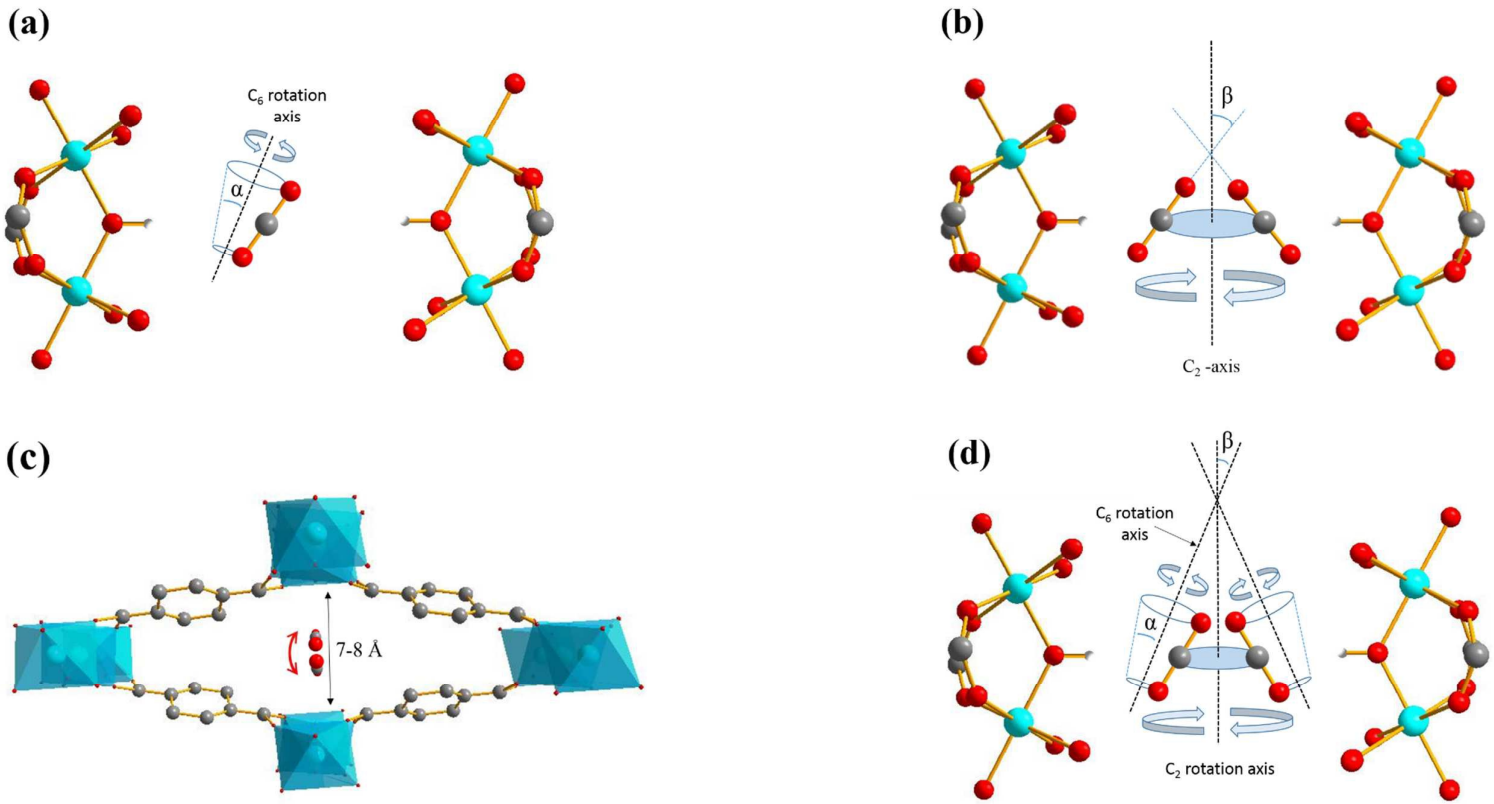

Fig. 3 The localized C_6 rotation, or wobbling, of CO_2 with a rotation angle α is shown in (a). An illustration of how CO_2 hops between the closest two adsorption sites with the hopping angle β between the longitudinal axis of CO_2 and the C_2 rotation axis is provided in (b). A schematic of how illustrates how CO_2 hops between the closest two adsorption sites in the *xy* plane in MIL-53 is shown in (c). The combination of wobbling (C_6 rotation, α) and two-site hopping (C_2 rotation, β) is depicted in (d). The colors red, grey, white and blue correspond to oxygen, carbon, hydrogen and the metal center, respectively.

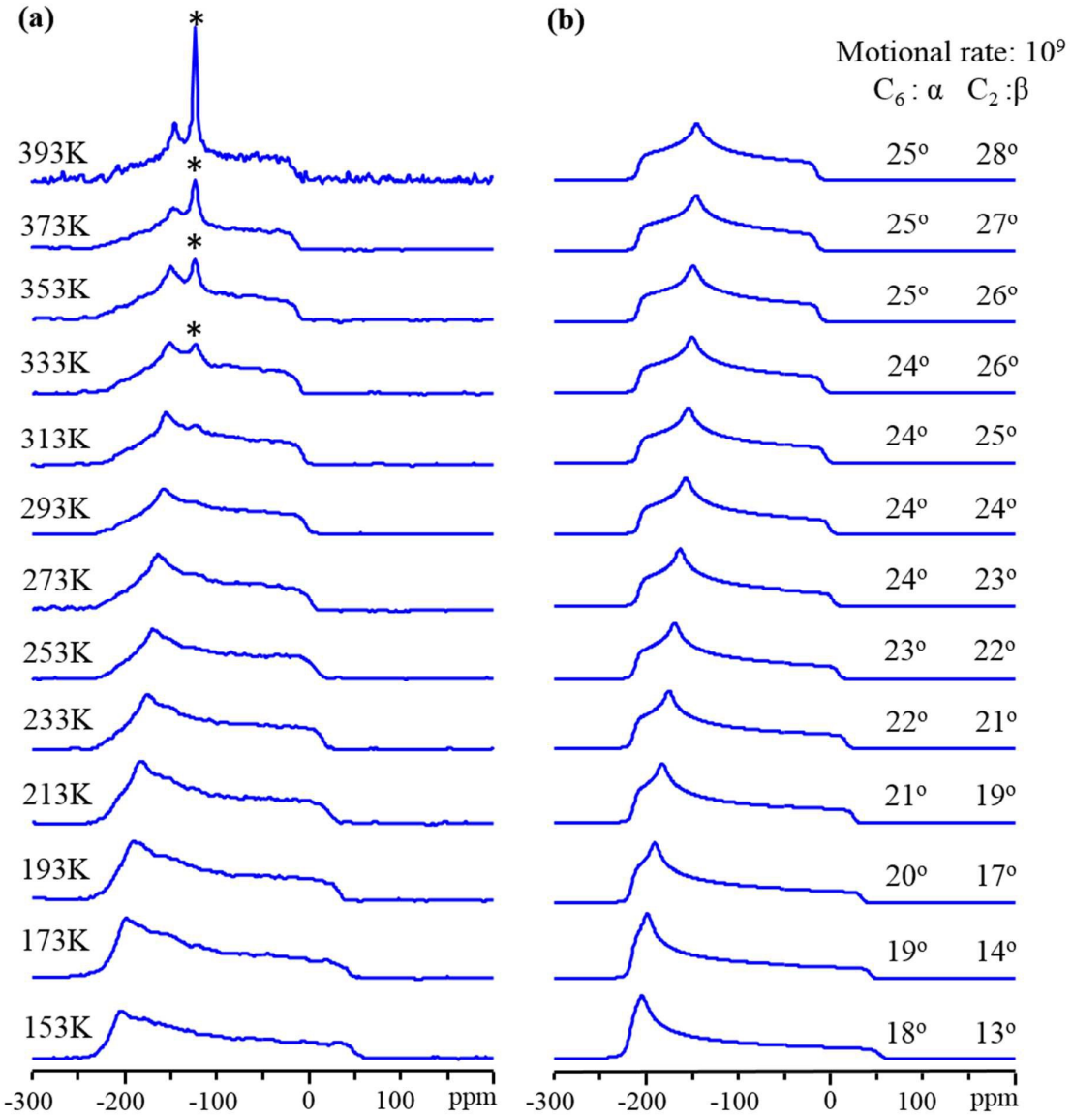

Fig. 4 The experimental and simulated static ^{13}C SSNMR spectra of CO_2 adsorbed within MIL-53 (Ga) are illustrated in (a) and (b), respectively. The asterisk (*) denotes a sharp resonance at high temperature that corresponds to gaseous, unbound CO_2. The simulated powder patterns were generated using the EXPRESS software and a fast rate of motion (10^9 Hz) for both dynamic modes. CO_2 adsorbed in MIL-53 (Ga) has same motions as CO_2 within MIL-53 (Al), which is a localized wobbling (C_6 with rotation angle α) and a non-localized two-site hopping (C_2 with rotation angle β) between two adsorption sites. See Figure S4 (ESI) for uncropped spectra that clearly show the edges of each powder pattern. The uncertainty in α and β is estimated to be ± 0.5 °.

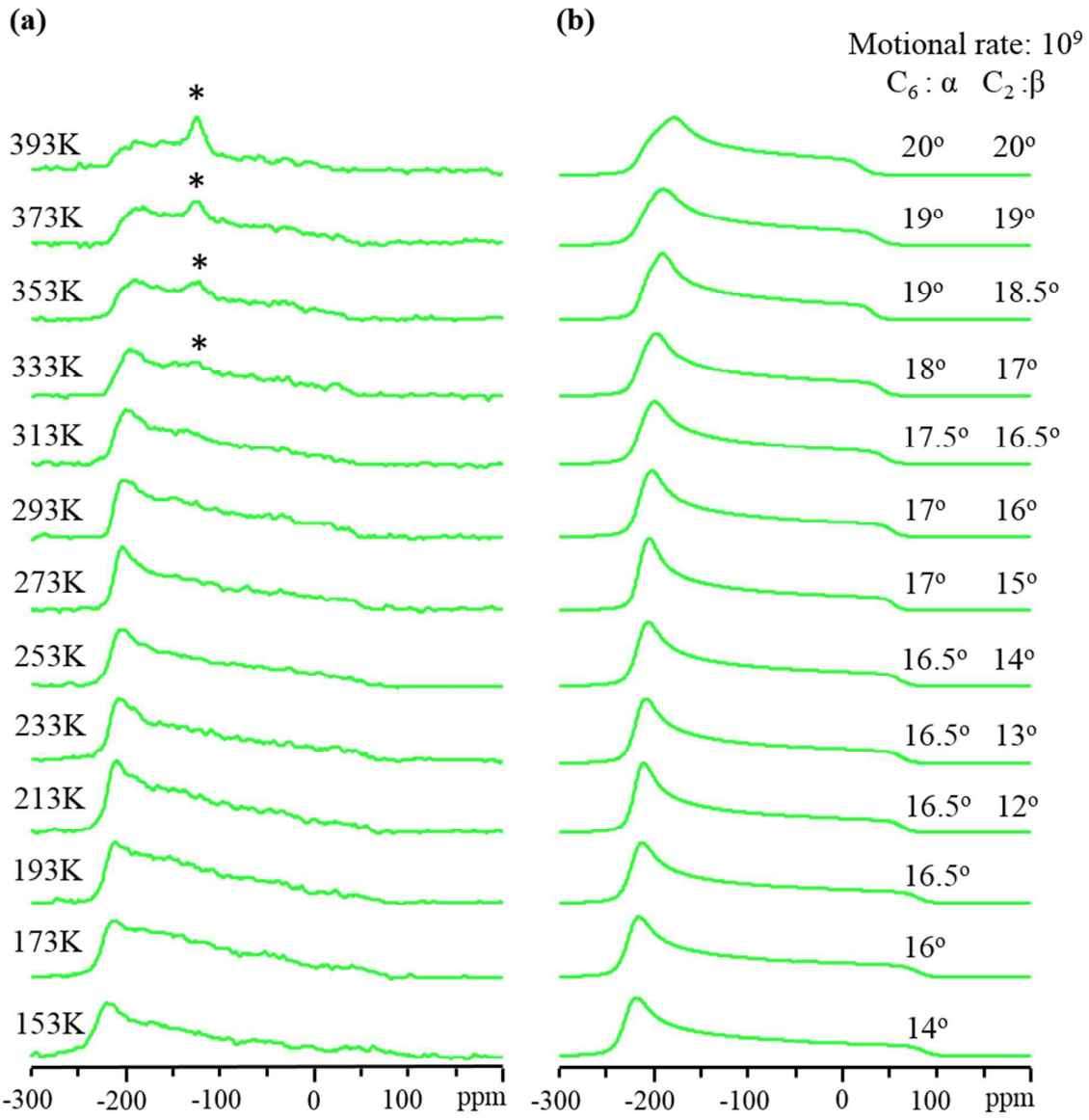

Fig. 5 The experimental static ^{13}C SSNMR spectra of adsorbed CO_2 within NH_2-MIL-53 (Al) are shown in (a) and simulated static ^{13}C SSNMR spectra are shown in (b). The simulated powder patterns were generated using the EXPRESS software and a fast rate of motion (10^9 Hz) for both dynamic modes. The C_6 motion (six-fold rotation) and α describe localized wobbling of CO_2 about the adsorption site, while the C_2 motion and β refer to a non-localized two-fold hopping between two adsorption sites. The asterisk (*) denotes a sharp resonance at high temperature that corresponds to gaseous, unbound CO_2. See Figure S5 (ESI) for uncropped spectra that clearly show the edges of each powder pattern. The uncertainty in α and β is estimated to be ±0. 2°.

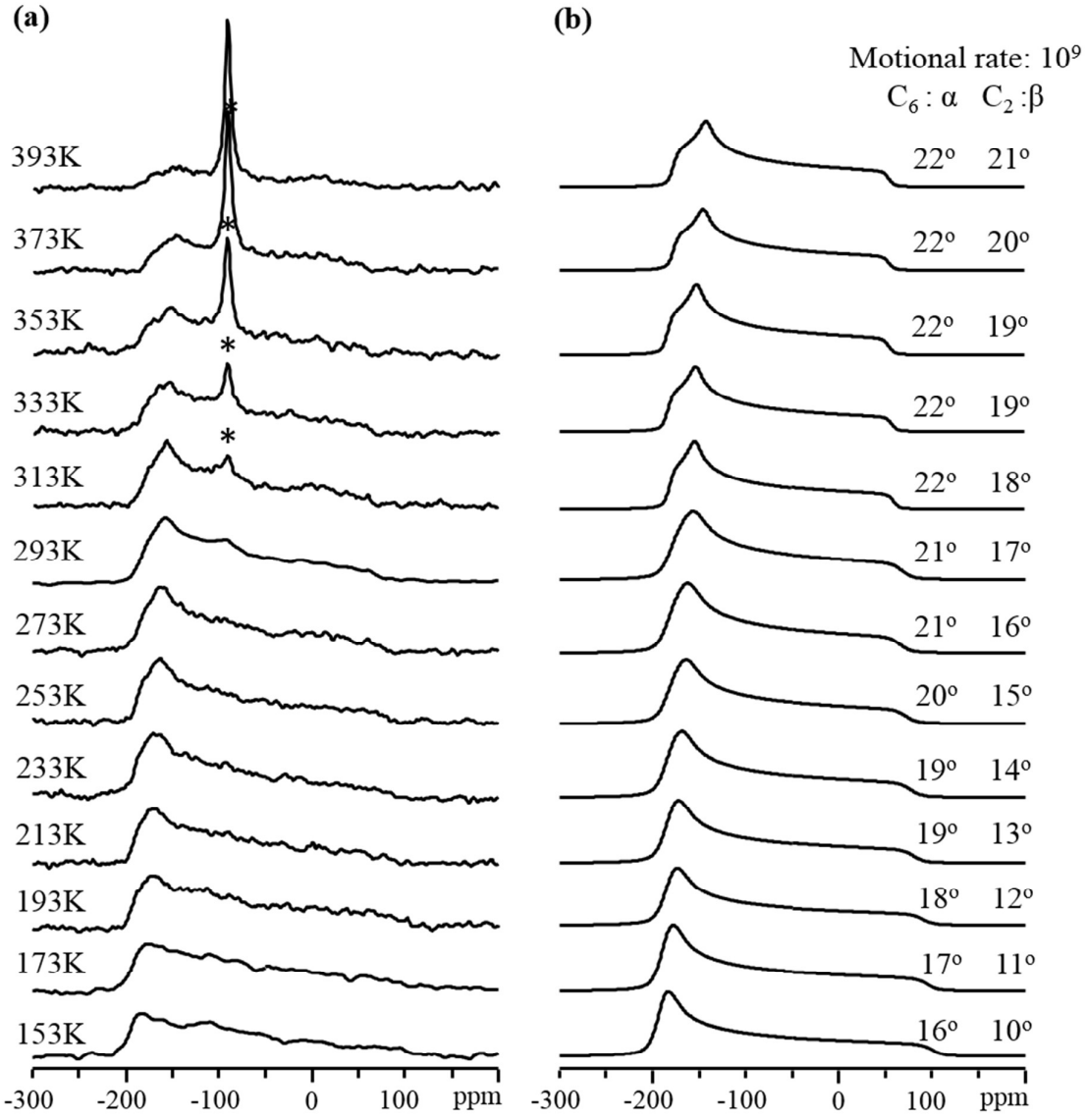

Fig. 6 The experimental and simulated static ^{13}C SSNMR spectra of adsorbed CO_2 within NH_2-MIL-53 (Ga) are shown in (a) and (b) respectively. The simulated powder patterns were generated using the EXPRESS software and a fast rate of motion (10^9 Hz) for both dynamic modes. The C_6 motion (six-fold rotation) and α describe localized wobbling of CO_2 about the adsorption site, while the C_2 motion and β refer to a non-localized two-fold hopping between two adsorption sites. The asterisk (*) denotes a sharp resonance at high temperature that corresponds to gaseous, unbound CO_2. See Figure S6 (ESI) for uncropped spectra that clearly show the edges of each powder pattern. The uncertainty in α and β is estimated to be ±0.2°.

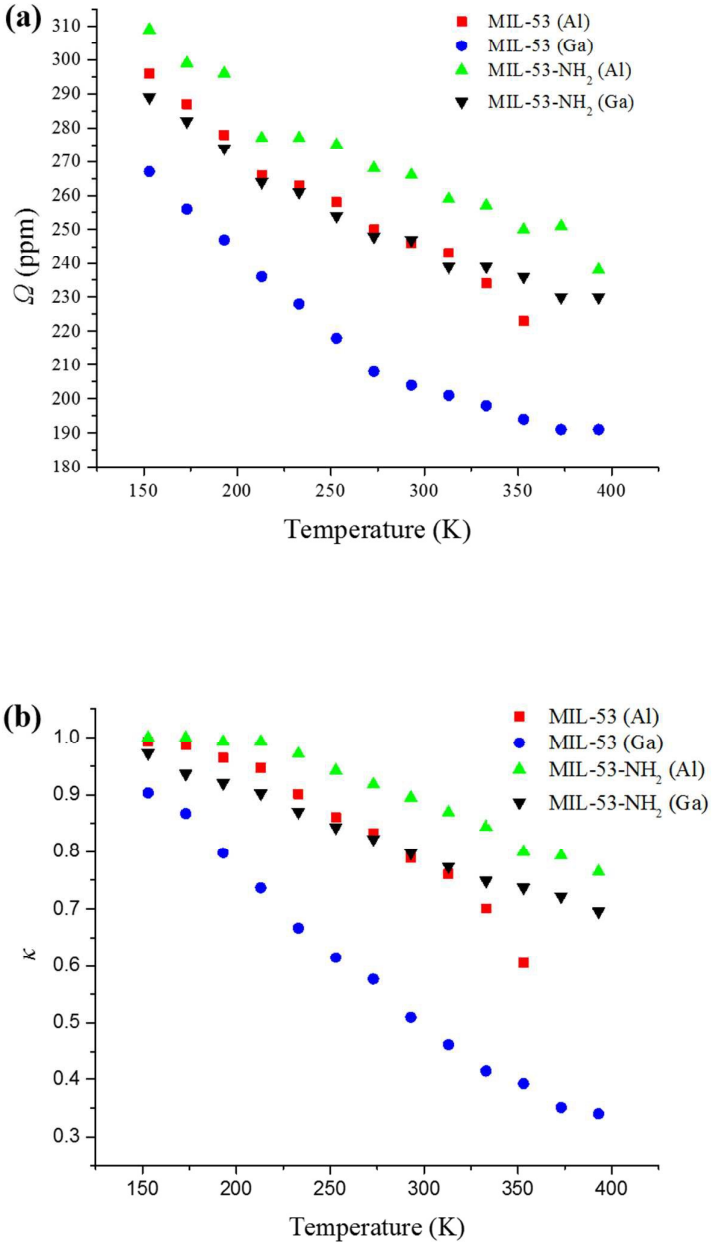

Fig. 7 A comparison of ^{13}C span (Ω) and skew (κ) NMR parameters corresponding to of CO_2 adsorbed in different MIL-53 MOFs across temperature from 153 K to 393 K are shown in (a) and (b), respectively.

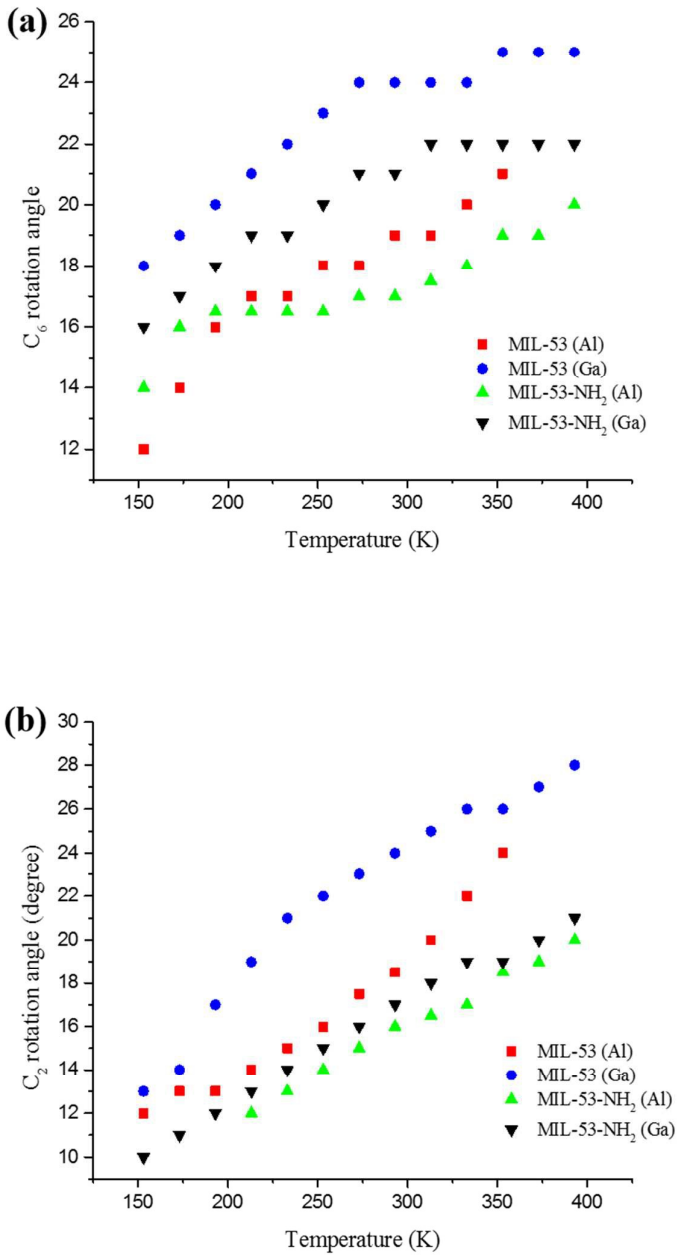

Fig. 8 A comparison of C_6 rotation angle (α) describing local wobbling in MIL-53 across temperatures from 153 K to 393 K is shown in (a) and a graph of the C_2 rotation angle (β) corresponding to non-localized hopping of CO_2 versus temperature is depicted in (b).

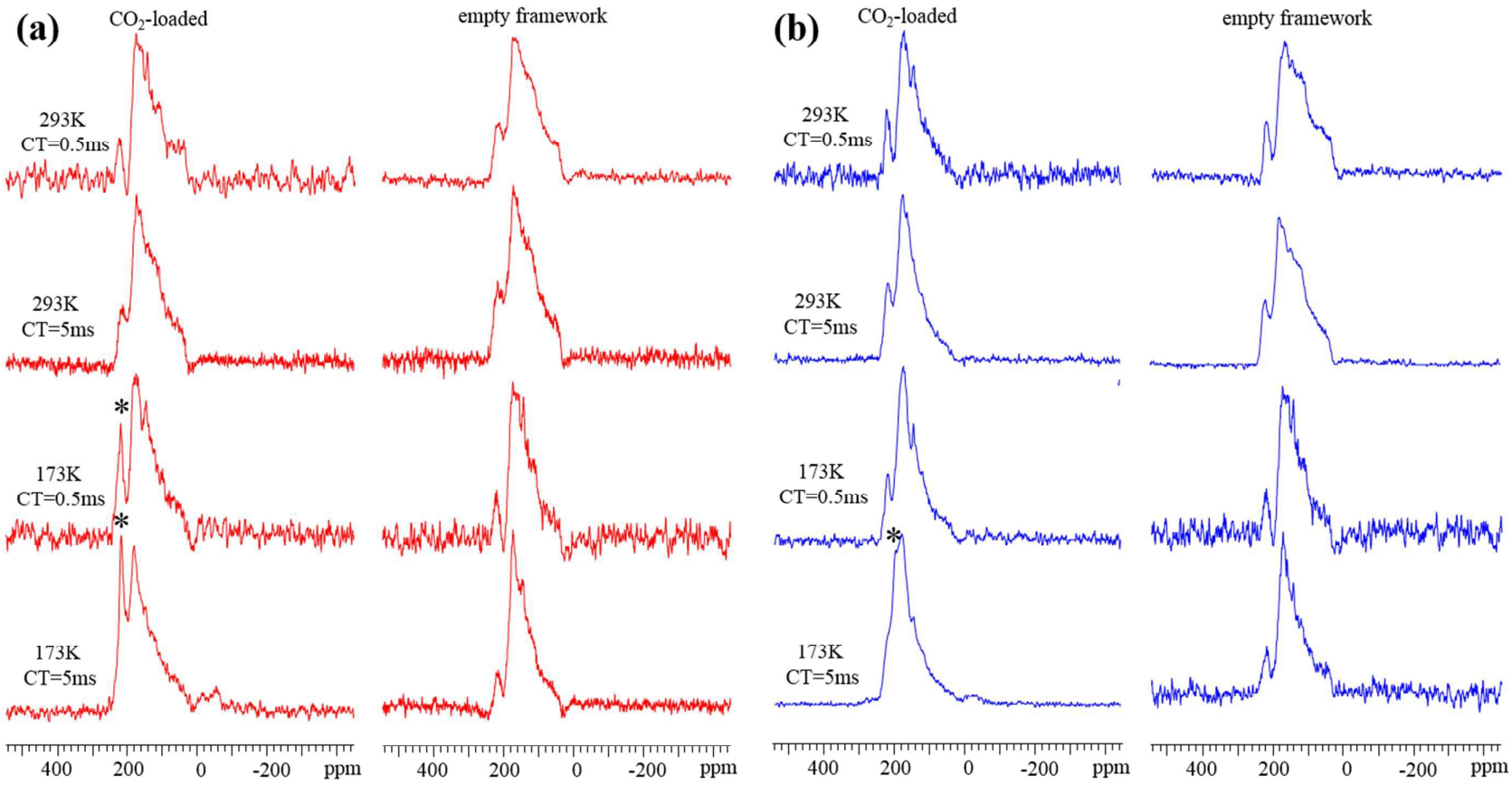

Fig. 9 Static ^{1}H-^{13}C CP SSNMR spectra of MIL-53 (Al) and MIL-53 (Ga) are shown in (a) and (b), respectively. Spectra of both CO_2 adsorbed samples and empty frameworks using different CP contact times (CTs) were acquired at 293 K and 173 K. The asterisk (*) denotes the resonance corresponding to adsorbed CO_2.

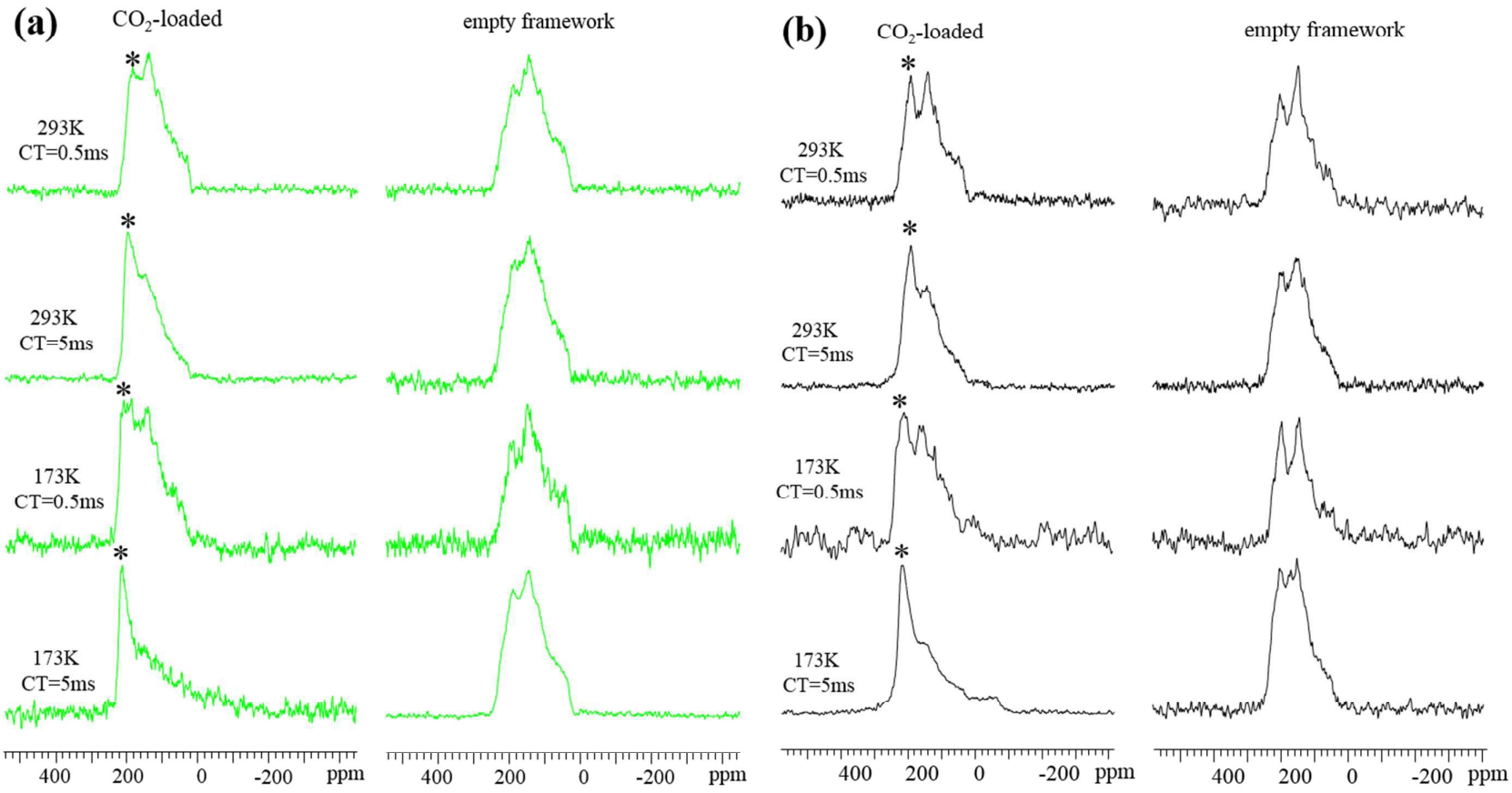

Fig. 10 ^{1}H-^{13}C static CP SSNMR spectra of NH_2-MIL-53 (Al) and NH_2-MIL-53 (Ga) are shown in (a) and (b), respectively. Spectra of both CO_2 adsorbed samples and empty frameworks with different contact time (CT) were acquired at 293 K and 173 K. The asterisk (*) denotes the resonance of adsorbed CO_2.

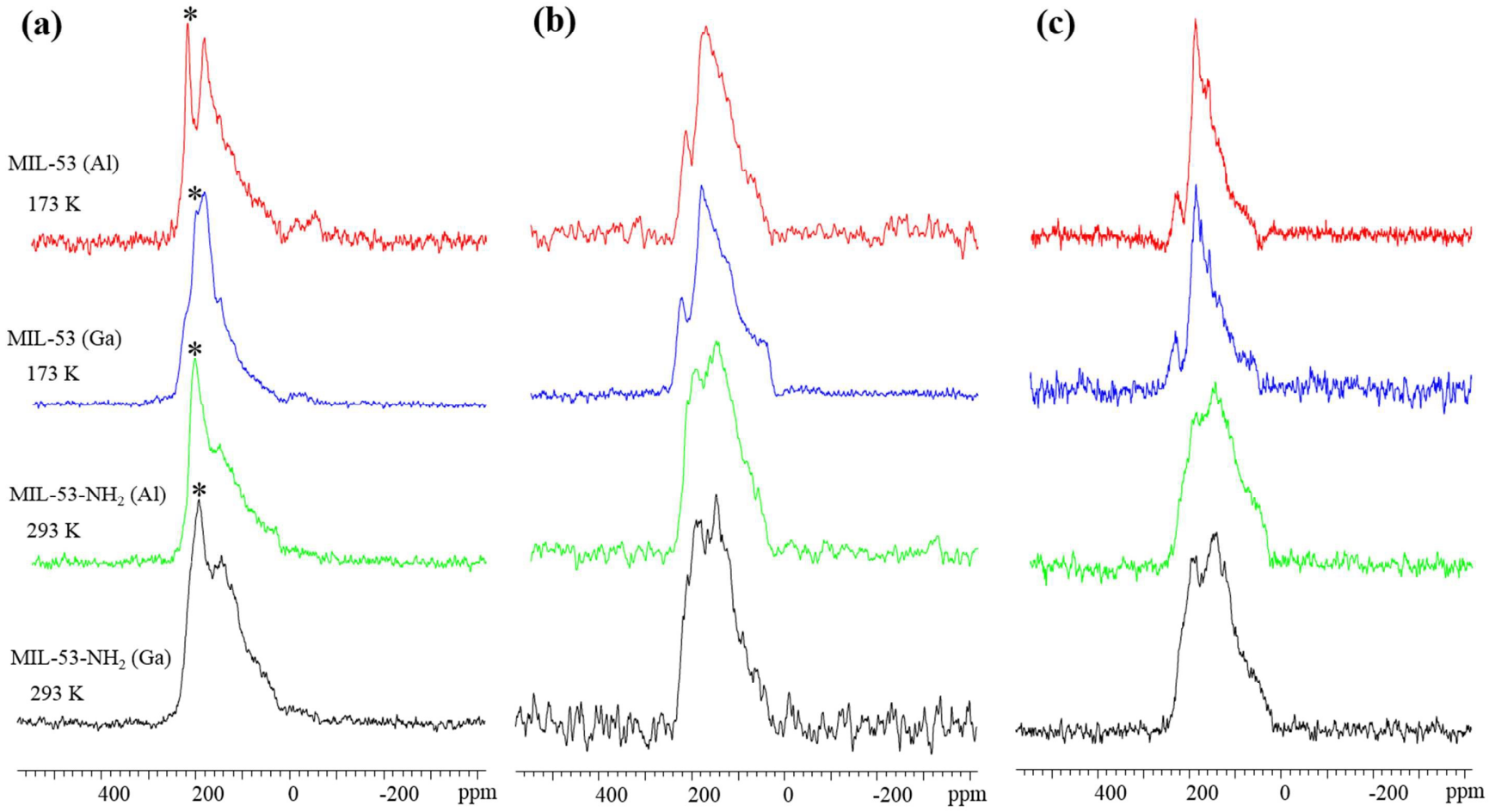

Fig. 11 Static ^{1}H-^{13}C CP SSNMR spectra of CO_2-loaded non-deuterated samples, CO_2-loaded deuterium exchanged samples and empty frameworks are shown in (a), (b) and (c), respectively. For MIL-53 (Al) and MIL-53 (Ga), the spectra were obtained at 173 K with CT = 5 ms, For MIL-53-NH_2 (Al) and MIL-53-NH_2 (Ga), the spectra were obtained at 293 K with CT = 5 ms. The asterisk (*) denotes the resonance of adsorbed CO_2.

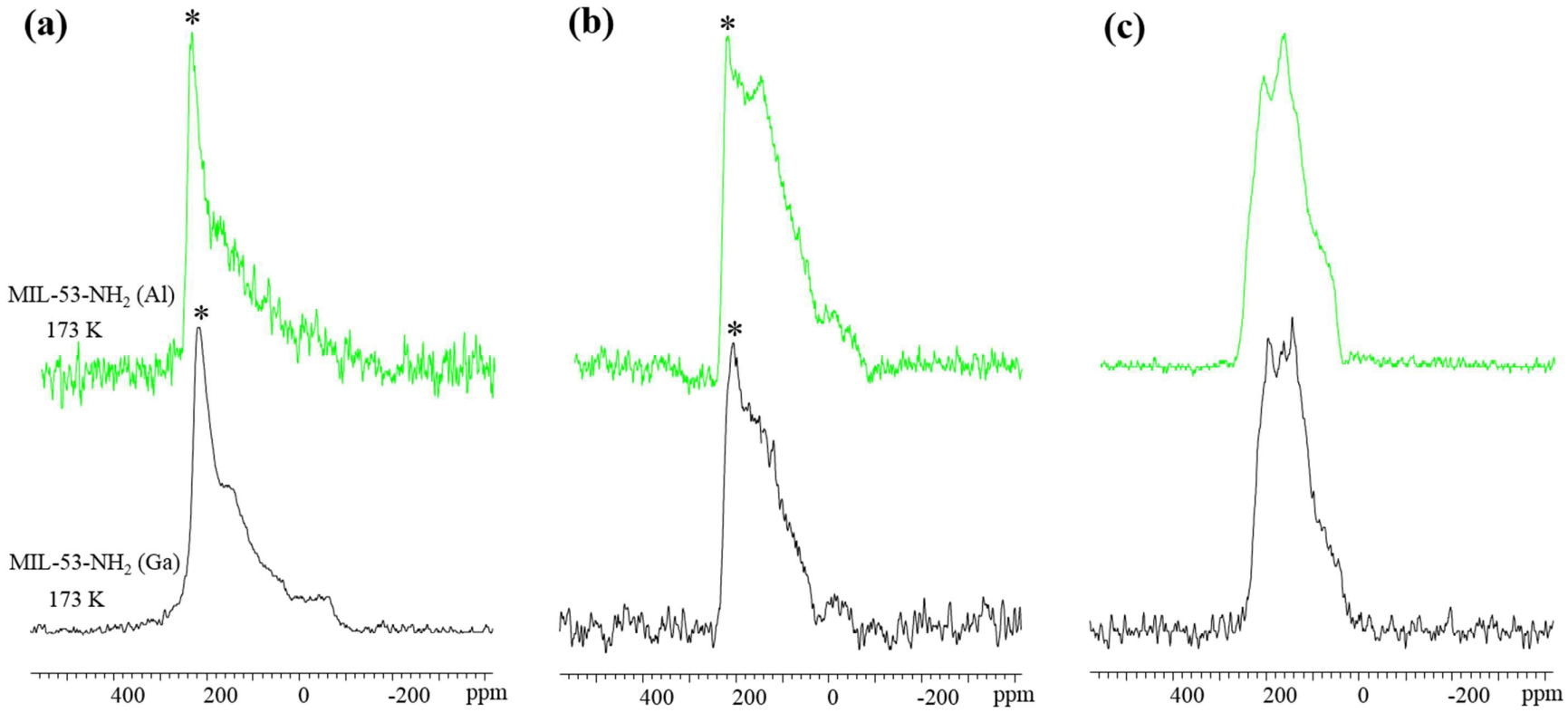

Fig. 12 ^{1}H-^{13}C CP SSNMR spectra of CO_2-loaded non-deuterated samples, CO_2-loaded deuterium exchanged samples and empty frameworks are shown in (a), (b) and (c), respectively. All the spectra were obtained at 173 K with CT = 5 ms. The asterisk (*) denotes the resonance of adsorbed CO_2.

TOC